

PONTIFICIA UNIVERSIDAD CATÓLICA DEL PERÚ

POSGRADUATE SCHOOL



**Development of an eco-friendly composite based on
geopolymer matrix produced with fired clay brick powder
and reinforced with natural fibers**

A thesis submitted for the degree of Master in Civil Engineering

by

Guido Leonardo Silva Mondragón

Supervisor

Suyeon Kim De Aguilar, PhD.

Co-Supervisors-Jurado- **Rafael Aguilar Velez, PhD.**

Jurado-**Javier Nakamatsu Kuniyoshi PhD.**

Lima, 2018

Abstract

Current construction industry is responsible for a large amount of greenhouse gas emissions due to the widespread use of building materials with high-embodied energy such as ordinary Portland cement-based materials and steel. Therefore, this thesis presents the development of a new eco-friendly building material based on a geopolymer matrix produced with Fired Clay Brick Powder (FCBP) and reinforced with natural fibers as a low CO₂ alternative for the traditional building materials.

With this purpose, a review of recent advances in the application of geopolymer composites and geopolymers reinforced with natural fibers in the construction industry were first presented. This review covers two major eco-friendly materials for construction: first, geopolymers obtained from industrial by-products and waste materials, such as fly ash, ground granulated blast furnace slag, construction and demolition wastes and main tailings; and second, natural fibers used as reinforcement for geopolymer composite materials. Literature review allowed the definition of morphology, size, and the molar ratio of SiO₂/Al₂O₃ in the raw material, together with the alkaline solution/solid ratio, NaOH concentration, SiO₂/M₂O molar ratio in the total alkaline solution and the curing conditions as key parameters in the formulation of geopolymers. It has been also found that the type, pre-treatment, amount and length of the natural fibers play an important role in the reinforcement of geopolymer matrices. Once key parameters of geopolymer composites production were identified, an attempt for the formalization of a methodology to improve the compressive strength of FCBP-based geopolymers is presented. The tests allowed the definition of optimum conditions of the FCBP-based geopolymers formulation and curing conditions, which resulted in a cementitious matrix with high compression strengths of up to 37 MPa. Nevertheless, high-strength geopolymers evidenced a fragile behavior and low ductility similar to Portland cement-based materials. Therefore, the last part of the work was focused on the evaluation of natural cellulose fibers (jute and sisal) as reinforcement of FCBP-based geopolymers. The results indicated that jute and sisal fiber addition at the optimum content significantly improved the compressive, splitting tensile and flexural strength with respect to the unreinforced geopolymer matrix and lead to a shifting of the failure mode from a brittle to a more ductile failure in all mechanical tests.

Acknowledgments

I want to express my gratitude to my supervisor Prof. Suyeon Kim and co-supervisors Prof. Rafael Aguilar and Prof. Javier Nakamatsu for all the support during these years and their help in the most difficult moments of this thesis. Furthermore, I would like to thank for the great opportunity to work in the Modification Materials research group (ModMat) and being part of the project “Development of eco-friendly composite materials based on geopolymer matrix and reinforced with waste fibers”.

I will be eternally indebted to Compañía Minera de Agregados Calcáreos S.A. (COMACSA) and its Research and Development Manager, Dr. Bruno Bertolotti for providing its facilities during the production stage. This thesis could not have been completed without their help.

I will also acknowledge to the National Council of Science, Technology and Innovation (CONCYTEC) for my postgraduate scholarship. I will also thank for supporting my research and funding my participation in an international congress.

My gratitude to my colleagues and friends David Castañeda, Alvaro Castañeda, Rosmery Naupari, Patricia Pórcel and Mauricio González for their support during my thesis. I am sure that our academic interactions and their advices help me to improve the quality of this thesis.

A special acknowledgment to my parents Guido and Aleyda and my sister Fiorella for their unconditional love. They taught me to live a plenty life and to be a better person with their example. Moreover, they also support me and were comprehensive in the most stressful passages during these two years. What I have achieved to this point is all thanks to them. Their advices guide my personal and professional life.

Content

Abstract	i
Acknowledgments	ii
Content	iii
List of Figures	v
List of Tables	vii
CHAPTER 1: Introduction	1
1.1. Motivation	2
1.2. Objectives	2
1.2.1. General objective	2
1.2.2. Specifics objectives.....	3
1.3. Organization	3
CHAPTER 2: A review of eco-friendly applications of natural fibers reinforced geopolymers	4
2.1. Introduction	5
2.2. Geopolymerization	7
2.3. Industrial by-products and waste materials for geopolymer production	9
2.3.1. Fly ash	9
2.3.2. Ground granulated blast furnace slag.....	12
2.3.3. Construction and demolition waste.....	14
2.3.4. Mine tailings.....	19
2.4. Natural fibers as reinforcement for geopolymer binders.....	20
2.4.1. Natural fibers.....	20
2.4.2. Plant fibers reinforcement for geopolymer matrices.....	24
2.4.3. Other natural fibers	28
CHAPTER 3: Analysis of the production conditions of geopolymer matrices from construction and demolition wastes	29

3.1.	Introduction	30
3.2.	Materials and Experimental plan	31
3.2.1.	Description of the raw materials	31
3.2.2.	Characterization of geopolymer matrices	33
3.2.3.	Preparation of samples	35
3.3.	Results and discussion	37
3.3.1.	Analysis of the effects of silica modulus (M_s)	37
3.3.2.	Analysis of the effects of the Na_2O content and optimization of the silica modulus (M_s)	38
3.3.3.	Optimization of water/binder ratio	42
3.3.4.	Optimization of oven curing conditions	43
CHAPTER 4: Natural cellulose fibers to improve the mechanical behavior of fired clay brick-based geopolymer composites		47
4.1.	Introduction	48
4.2.	Materials and Experimental plan	50
4.2.1.	Materials	50
4.2.2.	Research procedures	52
4.2.3.	Preparation of samples	54
4.3.	Results and discussion	55
4.3.1.	Tensile tests of fibers	55
4.3.2.	Compression tests of geopolymer composites	56
4.3.3.	Splitting tests of geopolymer composites	57
4.3.4.	Three-point bending tests of geopolymer composites	59
CHAPTER 5: Conclusions		62
5.1.	Conclusions	63
References		66

List of Figures

Figure 2.1. Chemical structures of (A) cellulose and (B) lignin.	32
Figure 2.2. Classification of natural plant fibers.....	32
Figure 3.1. Particle size distribution and morphology of FCBP: (a) Granulometric curves envelope of grinded raw material and (b) SEM micrograph.	32
Figure 3.2. X-ray diffractograms of FCBP. Q: Quartz (SiO_2); H: Hematite (Fe_2O_3); P: Plagioclase (albite/anortite, $(\text{Ca}, \text{Na})\text{Al}_2\text{Si}_2\text{O}_8$); A: Actinolite ($\text{Ca}_2(\text{Mg}_{4.5-2.5}\text{Fe}_{0.5-2.5})\text{Si}_8\text{O}_{22}(\text{OH})_2$); M : Microcline ($\text{KAl}_2\text{Si}_2\text{O}_8$); C: Calcite (CaCO_3); K: Orthoclase/Microcline ($\text{KAl}_2\text{Si}_2\text{O}_8$).	33
Figure 3.3. Mechanical characterization of geopolymer matrices to uniaxial compression: (a) Schematic view of the compression test; (b) Schematic view of the silicon molds and (c) Resulting geopolymer cubic sample. (units in mm).....	34
Figure 3.4. Production process of geopolymers: (a) FCBP; (b) FCBP geopolymer paste; (c) FCBP-based geopolymer cubic sample.....	36
Figure 3.5. Effect of silica modulus (M_s): (a) Density and (b) 7 th -day compressive strength.....	38
Figure 3.6. Effect of Na_2O content for a given M_s : (a) Density and (b) 7 th -day compressive strength.....	40
Figure 3.7. FT-IR spectra of unreacted FCBP and FCBP- based geopolymers with different Na_2O contents.....	41
Figure 3.8. Effect of the water/binder ratio: (a) Density and (b) 7 th -day compressive strength.....	43
Figure 3.9. Effect of oven curing time on the 7 th -day compressive strength for a given oven curing temperature: (a) Density; (b) 7 th -day compressive strength.	44
Figure 3.10. Compression stress vs. strain curves and failure modes for a given oven curing time of FCBP-based geopolymers.	45
Figure 3.11. FT-IR spectra of unreacted FCBP and FCBP-based geopolymers cured for different oven curing time periods.	46
Figure 4.1. Natural fibers used as reinforcement of FCBP-based geopolymer matrix: (a) Jute fiber and (b) Sisal fiber.....	51
Figure 4.2. Particle size distribution and morphology of FCBP: (a) Granulometric curves envelope and (b) SEM micrograph.....	52

Figure 4.3. Mechanical characterization: (a) Tensile test of single fibers; (b) Universal testing machine used in mechanical characterization of geopolymer composites; (c) Geopolymer composite cubic sample; (d) Compression test; (e) Geopolymer composite cylindrical sample; (f) Splitting tensile test; (g) Geopolymer composite prismatic sample; (h) Three-point bending test. Units in mm. 53

Figure 4.4. Micrographs of fresh geopolymer composites: (a) Control matrix; (b) Jute-FRGC; and (c) Sisal-FRGC. 54

Figure 4.5. Tensile test of single jute and sisal fibers: (a) Tensile strengths; (b) Tensile stress vs strain curves. 56

Figure 4.6. Compression test results for fiber-reinforced geopolymer composites: (a) 7th-day compressive strengths of specimens reinforced with jute and sisal fibers; (b) Compression vs. strain curves; (c) Failure mode of control matrix; (d) Failure mode of jute-FRGC (1.5% fiber content); and (e) Failure mode of sisal-FRGC (2.5% fiber content)..... 57

Figure 4.7. Splitting test results for fiber-reinforced geopolymer composites: (a) 7th-day splitting tensile strengths in specimens reinforced with jute and sisal fibers; (b) Tensile stress vs displacement curves; (c) Failure mode of control matrix; (d) Failure mode of jute-FRGC (1.5% fiber content); and (e) Failure mode of sisal-FRGC (2.5% fiber content) 59

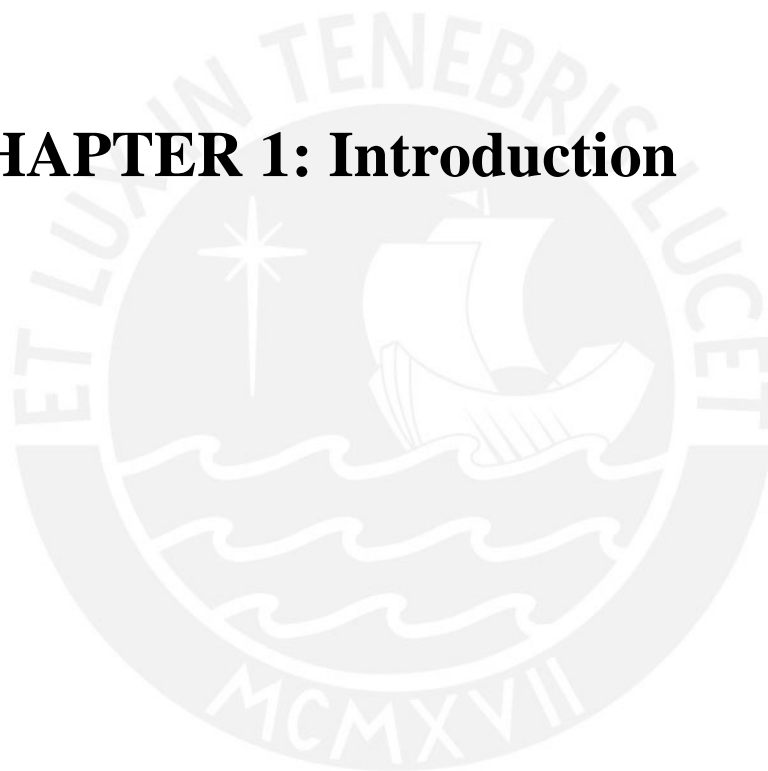
Figure 4.8. Three-point bending test results of fiber reinforced geopolymer composites: (a) 7th-day flexural strengths in specimens reinforced with jute and sisal fibers; (b) Flexural stress vs displacement curves; (c) Failure mode of control matrix; (d) Failure mode of jute-FRGC (2% fiber content); (e) Failure mode of sisal-FRGC (3% fiber content); and (f) Bridging of fibers across crack in sisal-FRGC (3% fiber content)..... 61

List of Tables

Table 2.1. Types of geopolymers depending on the Si:Al ratio.....	8
Table 2.2. Reported mixtures for fly ash-based geopolymer pastes and mortars.	12
Table 2.3. Reported mixtures for GGFBS-based geopolymer pastes and mortars. ...	14
Table 2.4. Reported mixtures for clay brick powder-based geopolymer pastes and mortars.....	17
Table 2.5. Reported mixtures for CWP-based geopolymer pastes and mortars.	18
Table 2.6. Reported mixtures for MT-based geopolymer pastes and mortars	20
Table 2.7. Reported studies regarding plant short-fiber reinforced geopolymer composites.....	26
Table 2.8. Reported studies regarding plant fabric reinforced geopolymer composites.....	28
Table 2.9. Reported studies regarding other natural fibers reinforced geopolymer composites.....	28
Table 3.1. Chemical composition of FCBP by X-ray fluorescence spectroscopy	32
Table 3.2. IR bands and their corresponding bond vibration present in FCBP-based geopolymers.	35
Table 3.3. Experimental plan for the optimization of FBCP-based geopolymers production.	37
Table 4.1. Chemical composition of FCBP by X-ray fluorescence spectroscopy	52
Table 4.2. Summary of mixture proportions used for preparation of the control matrix and FRGCs.....	55



CHAPTER 1: Introduction



1.1. Motivation

Unsustainability is one of the main features of the modern construction industry. This industry contributes with 30% of the worldwide carbon dioxide (CO₂) emissions and is the largest consumer industry of raw materials, approximately 50% by weight (Pacheco-Torgal & Jalali, 2012). This is largely due to the widespread use of Ordinary Portland cement (OPC) to produce OPC-based materials as concrete and mortars for modern buildings and infrastructures. The global cement production was estimated in around 4.1 billion metric tonnes in 2016, and China accounted for more than 50% of the total production (U.S. Geological Survey, 2017). Processes as calcination of limestone and fuel combustion plus mining, grinding and transportation during OPC production require enormous amounts of energy and release great quantities of greenhouses gases (Gartner, 2004). It is estimated that each tonne of OPC generates the same mass of CO₂ and requires about 110 KWh of electricity because clinker formation requires high temperatures (Imbabi et al., 2012; Krishnan et al., 2014). Since OPC-based materials exhibit a brittle behavior, OPC concretes are traditionally reinforced by the addition of steel bars producing a composite material with enhanced ductility. However, steel bar reinforcement is highly expensive and its corrosion is the main reason of structure deterioration. Steel bar reinforcement also presents a disadvantage from an environmental point of view due to its production is responsible for the 31% of the CO₂ emission of reinforced concrete (Gorkum, 2010; Pacheco-torgal & Jalali, 2011). Therefore, this thesis purports to be an answer for the global concern related to the searching of alternative building materials. The development of an eco-friendly composite material based on a geopolymer matrix and reinforced with natural fibers is proposed. A geopolymer matrix produced from recycled fired clay brick powder, a construction and demolition waste, is presented. Moreover, jute and sisal natural fibers are explored as a low CO₂ reinforcement of the geopolymer matrix to improve its mechanical properties making it suitable for the construction industry.

1.2. Objectives

1.2.1. General objective

The objective of this thesis is the development of an eco-friendly composite material based on a geopolymer matrix produced with fired clay brick powder and reinforced with natural fibers.

1.2.2. Specifics objectives

- i. Generate a document that presents a review of the recent advances in the development of geopolymer matrices and geopolymers reinforced with natural fibers
- ii. Find the optimum alkaline activating solution and best curing conditions for the production of fired clay brick powder-based geopolymers
- iii. Explore the use of short sisal and jute fibers as reinforcement of fired clay brick powder based-geopolymers

1.3. Organization

This thesis is composed by five chapters. Chapter 1 presents the motivation and importance of the research work. Moreover, this chapter introduces the general and specifics objectives as well as a description of the organization of this document that includes a brief explanation of the content of each chapter. Chapter 2 presents the state of the art of the application of geopolymer matrices and natural fiber reinforced geopolymer composites in the construction industry. This review chapter focuses on the two components of fiber-reinforced geopolymer composites: (1) geopolymers produced with a wide range of industrial by-products and wastes materials; and (2) natural fibers used as short and layer reinforcement of geopolymer composite materials. Chapter 3 deals with the optimization of the compressive strength of fired clay brick powder (FCBP)-based geopolymers. The optimization methodology is based on studying the effect of the alkaline activating solution and curing conditions by changing the sodium oxide (Na_2O) content, the $\text{SiO}_2/\text{Na}_2\text{O}$ molar ratio, the water/binder ratio, the oven curing temperature and oven curing time. Chapter 4 presents the mechanical characterization of jute and sisal fiber reinforced geopolymer composites. Unreinforced and reinforced FCBP-based geopolymer samples with different contents of jute and sisal fibers were tested under compression tests, splitting tensile tests and three-point bending tests to study the influence of the fiber content and fiber type on the mechanical properties of geopolymer composites. Finally, Chapter 5 presents the conclusions of the thesis and discusses possible future works.

CHAPTER 2: A review of eco-friendly applications of natural fibers reinforced geopolymers

Abstract. The construction industry is responsible not only for the consumption of huge amounts of natural resources but also for the emission of a large quantity of CO₂ gas. In this regard, geopolymers have emerged as an environmentally friendly alternative for conventional construction materials, like Portland cement, since they reduce greenhouse gas emissions and use industrial wastes. A review of recent advances in the application of geopolymer composites and geopolymers reinforced with natural fibers in the construction industry is presented and it covers two major eco-friendly materials for construction: first, geopolymers obtained from industrial by-products and waste materials, such as fly ash, ground granulated blast furnace slag, construction and demolition wastes and main tailings; and second, natural fibers used as reinforcement for geopolymer composite materials. Several reports have studied the effect of adding plant fibers, such as pineapple leaf, sisal, linen, flax, cotton, among others, to fly ash geopolymers. It has been found that the type, pre-treatment, amount and length of the natural fibers play an important role in the reinforcement of geopolymer matrices. Moreover, layer reinforcement using woven and non-woven fabrics of natural fibers seem to be more effective than short fibers randomly oriented.

2.1. Introduction

The search for alternative building materials has gained great attention due to the unsustainability of the modern construction industry. This industry accounts for 30% of global carbon dioxide (CO₂) emissions and consumes more raw materials than any other industry, nearly 50 % by weight (Pacheco-Torgal & Jalali, 2012). Ordinary Portland cement (OPC) is widely used in this industry for the production of conventional mortar and concrete which are needed for modern buildings and infrastructures due to their versatility and highly reliable performance, and also their widespread availability and comparatively low cost of raw materials and processing technologies (Matheu et al., 2015; Zhang et al., 2014). In 2016, the total estimated worldwide cement production reached around 4.1 billion metric tonnes, which was a slight increase compared to the previous year, and more than 50 % of the total production is attributed to China (U.S. Geological Survey, 2017). OPC production requires enormous amounts of energy and releases huge quantities of greenhouse gases mainly due to the calcination of limestone and fuel combustion in addition to mining, grinding and transportation (Gartner, 2004). Even though it depends on the type of cement and the process used, it is estimated that each tonne of OPC generates roughly the same mass of CO₂ to the environment (Imbabi et al., 2012; Krishnan et al., 2014), and requires 60–130 kg of fuel oil or an equivalent and about 110 KWh of electricity since its production requires temperatures well above 1000°C for clinker formation (Imbabi et al., 2012). Due to the high CO₂ emissions and energy consumption, alternative construction materials are being investigated.

In this regard, geopolymers, which can be made from locally available minerals or recycled or waste materials that come from industry, agriculture and domestic sources, are perfect candidates that have attracted the construction industry interest (Das et al., 2014; Imbabi et al., 2012). Geopolymers are produced from materials that are rich in silico-aluminates, which is an advantage since more than 65% of the Earth's crust consists of Al-Si minerals (NPCS Board of Consultants & Engineers, 2008). This relatively new inorganic polymer, developed by Davidovits (1991), emerges as a promising alternate binder in replacement of OPC paste. The synthesis of geopolymers requires an alkaline activation of the alumino-silicates raw materials in order to form new Si-O-Al and Si-O-Si networks (Davidovits, 1991). As mentioned above, these raw materials can be industrial by-products such as fly ash (FA), ground granulated

blast furnace slag (GGBFS), rice husk ash (RHA), palm oil fuel ash (POFA), among others (Chen et al., 2014; Cheng & Chiu, 2003; He et al., 2013; Salih et al., 2014). In this way, a value is given to otherwise waste and potentially problematic materials. Furthermore, several studies have been reported on the production of geopolymers based on waste materials as copper and tungsten mine tailings (MT), concrete demolition waste and fired clay brick powder (Ahmari et al., 2012; Pacheco-Torgal et al., 2009; Vásquez et al., 2016; Zawrah et al., 2016). The substitution of OPC with geopolymers could result in an 89% decrease in CO₂ emissions for each ton of OPC (Davidovits, 1993). With the development of these inorganic alumino-silicate polymers, new alkali activated inorganic cementitious compositions have already been commercially introduced into the US market (Davidovits, 1994).

Geopolymers have not only environmental advantages compared to OPC based materials but can also have superior mechanical properties and better resistance to fire, sulfates and acids (Singh et al., 2015). However, as OPC products, geopolymers can show a brittle failure due to its low tensile strength that could impose several constraints and limitations in a possible structural design. Traditionally, OPC concretes are reinforced by means of the addition of steel bars producing a composite material with ductile behavior. However, steel reinforcement has several disadvantages: steel bar corrosion is the main reason of structure deterioration, is highly expensive, and its production is responsible for the 31% of the CO₂ emission of reinforced concrete (Gorkum, 2010; Pacheco-torgal & Jalali, 2011). Several investigations have proposed the use of micro and macro synthetic and natural fibers to reinforce cementitious materials (Pacheco-torgal & Jalali, 2011). Although both types of fibers have shown promising results in geopolymer pastes (Korniejenko et al., 2016; Korniejenko et al., 2015), natural fibers are more eco-friendly and have lower density, higher specific strength and lower costs than synthetic fibers, and do not require high energy consuming process for their fabrication (Chen et al., 2014).

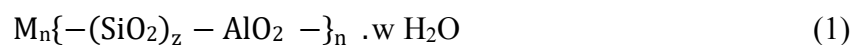
In this way, the use of by-products and waste materials for the production of geopolymers reinforced with natural fibers could become a sustainable construction system. These composite materials could have high mechanical and durability properties and at the same time leave a low carbon footprint. This review paper compiles research information of materials used in the production of natural fiber reinforced geopolymers for the production of eco-friendly building materials. Section

2 presents the basics of geopolymer formation, Section 3 includes the different silico-aluminate resources used for geopolymer production and Section 4 focuses on natural fibers that have been studied as reinforcement of geopolymer matrices.

2.2. Geopolymerization

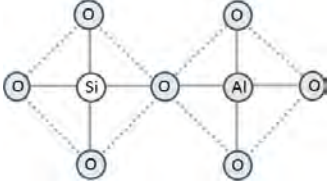
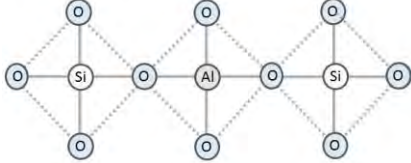
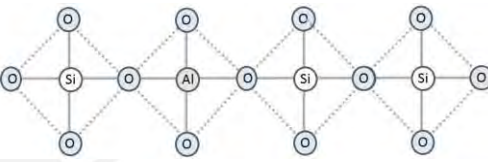
Davidovits found that silicon and aluminium-containing minerals can react chemically in alkaline conditions and form polymeric chains and crosslinked networks consisting of Si-O-Al-O bonds (Das et al., 2014; He et al., 2013). Geopolymers are the product of this polymerization reaction that involves Al-Si rich materials with an alkaline activating solution, such as sodium hydroxide (NaOH) or potassium hydroxide (KOH), usually with the addition of sodium silicate (Na₂SiO₃) or potassium silicate (K₂SiO₃) aqueous solutions (Das et al., 2014). Geopolymerization relies on the capacity of the aluminum ion to induce crystallographic and chemical changes in a silica backbone (with different coordination numbers 4 to 6) (Davidovits, 2005). The chemical composition of geopolymers are similar to natural zeolitic materials and thus geopolymers are considered as inorganic polymers, however, geopolymers are amorphous to semi-crystalline whereas zeolites are crystalline in nature. In addition to this, zeolites usually form in closed hydrothermal systems but geopolymers do not (Abdullah et al., 2017; Khale & Chaudhary, 2007).

Geopolymers are also known as polysialates, where the term “sialate” is derived from silicon-oxo-aluminate. The three-dimensional network consists of tetrahedral units of SiO₄ and AlO₄ linked together, sharing oxygen atoms. The structure also contains cations, usually sodium, potassium, lithium, calcium, barium, ammonium or hydrogen, to counterbalance the negative charges due to the aluminate units, AlO₄ (Khale & Chaudhary, 2007). The empiric formula of the polysialate is shown in eq. (1).



where M is the cation, n is the degree of polymerization, z is an integer (usually 1, 2 or 3) and w is the number of water hydration molecules in the network (Davidovits, 1979). Table 2.1 shows the types of geopolymers, poly(sialate), poly(sialate-siloxo) and poly(sialate-disiloxo), ideally formed depending on the Si:Al ratio.

Table 2.1. Types of geopolymers depending on the Si:Al ratio (adapted and modified from Brus et al. (2016))

Si:Al ratio	Chemical formation	Graphical representation
1	Poly(sialate) -Si-O-Al-O-	
2	Poly(sialate-siloxo) -Si-O-Al-O-Si-O-	
3	Poly(sialate-disiloxo) -Si-O-Al-O-Si-O-Si-O-	

According to Silva et al. (2007), the geopolymerization process can be divided into three main phases: (i) dissolution of the oxidized minerals present in the raw material (usually silica and alumina) under highly alkaline conditions, (ii) transport/orientation of the dissolved oxidized minerals followed by coagulation and gel formation and (iii) polycondensation to form a three dimensional network of aluminosilicate structures. Although there is some controversy in this respect, geopolymers are also called alkaline-activated aluminosilicate binders or alkaline-activated cementitious materials by some researchers (Jian-Xiong et al., 2004). Theoretically, any pozzolanic compound or material with high content of alumina and silica is suitable for geopolymer synthesis in strongly alkaline conditions.

There are many factors that need to be considered for the geopolymerization reaction, in the first place, the physical characteristics and chemical composition of the raw material will determine the alkaline degree of the activator. Since raw materials are very different and could also change from batch to batch (mineral or waste materials, for example), it is important to fully characterize the samples and, according to this, optimize the composition and amount of the activating solution. For example, Błaszczyszki and Król (2017) have reported the difference in properties of geopolymers of calcareous and siliceous fly ash when the activating solution composition and the molar ratio of $\text{SiO}_2/\text{Na}_2\text{O}$ were varied. The activating solution

composition and concentration greatly affected the compressive strength of the product since the dissolution of Si^{4+} and Al^{3+} ions from the source material and the formation of sodium and potassium aluminosilicates was different with each formulation. The authors proposed that an increase in Si and Al dissolution and more aluminosilicate formation occurred with a higher concentration of activating solution, which leads to an increase in compressive strength. Villa et al. (2010) studied the influence of the $\text{Na}_2\text{SiO}_3/\text{NaOH}$ ratio (from 0.4 to 15.0) in natural zeolite based geopolymers and obtained a maximum compressive strength with a ratio of 1.5, they noted that when the ratio was increased to 5, 10 and 15 reduced the strength. The authors also evaluated the relation between curing conditions (temperature and time) with strength. They observed that when the curing temperature was high (60 and 80 °C), a short period of curing time favored high compressive strengths, while low curing temperatures required longer periods of time to acquire a significant increase in strength. Similar results were obtained in the study of palm oil boiler ash (Si – Ca binding) by Yahya et al. (2015). A maximum strength of 11.5 MPa was reached with a $\text{Na}_2\text{SiO}_3/\text{NaOH}$ ratio of 1.5, and a high curing temperature (80 ~ 90 °C).

2.3. Industrial by-products and waste materials for geopolymer production

2.3.1. Fly ash

Fly ash is a finely-grained inorganic powder produced during the combustion of pulverized coal in thermal power plants for electricity production (European Committee for Standardization, 2008; Querol et al., 2002). As global electricity production shows an important dependency on coal sources, enormous quantities of fly ash are produced around the world, e.g. the US alone produced 51 million tons of fly ash in 2014 (American Coal Ash Association, 2015). There are some applications for fly ash, however, the percentage of fly ash consumed is very low, so most parts of these ashes are dumped in landfills and storage lagoons resulting in potential land, environmental and human health issues (Diaz et al., 2010). In general, the shape of fly ash particles is spherical with a particle size ranging from less than 1 μm up to 150 μm (Thomas, 2011). ASTM standards regarding fly ash (ASTM, 2010) classifies this material based on its chemical composition resulting in two types of fly ashes: Class F and Class C. The chemical composition of fly ash varies depending on the coal source and the combustion process, but is mainly composed by SiO_2 and Al_2O_3 (Diaz

et al., 2010). Class F fly ash results typically from burning anthracite or bituminous coals, while Class C fly ash is produced when lignite and sub-bituminous coals are combusted (ASTM, 2010). The main difference between both types of fly ashes is that Class C fly ash has greater amounts of total calcium compounds than Class F fly ash (ASTM, 2010). In regards to geopolymer production, fly ash is an excellent raw material since it contains high amounts of silica and alumina. According to Fernández-Jiménez (2003), there are some characteristics of fly ash that produce a geopolymer with good binding properties: low CaO content i.e. fly ash Class F, less than 5% of unburned material; less than 10% Fe₂O₃ content ; between 40-50% of reactive silica; 80-90% of particles finer than 45 µm, as well as, having a high content of vitreous phases. However, it has been reported that geopolymers with high compressive strengths can also be produced with fly ash with a high content of CaO (see Table 2.2).

Table 2.2 summarizes the parameters studied to produce fly ash-based geopolymers and their compressive strengths that have been reported in the literature. A fly ash-based geopolymer paste with a compressive strength of 59 MPa was developed by Kong et al. (2007) by mixing class F fly ash with an alkaline solution made by sodium silicate and potassium hydroxide with a silica modulus of 1.2 ($M_s = \text{SiO}_2/\text{M}_2\text{O}$). The curing regime consisted of leaving sealed samples for 24 h at room temperature and then heating them up at 80 °C for another 24 h after which the samples were removed from their molds. Plastic films to seal geopolymer pastes to avoid moisture loss during curing were also used by Guo et al. (2010) who used vinyl films and made geopolymers from class C fly ash with a 28-day compressive strength of 63 MPa. They used an alkaline solution with $M_s = 1.5$ and cured the samples at 75°C for 8 hours and were left at 23 °C until the mechanical test. On the other hand, Palomo et al. (1999) used sealed containers to maintain a relative humidity close to 100% in the paste. They reported a fly ash-based geopolymer that showed a compressive strength of 68.7 MPa only after one day of casting. Therefore, it seems that keeping a high relative humidity using sealed molds or covering samples with films might be important and should be taken into account during curing of geopolymer pastes. Somna et al. (2011) reported geopolymers made of fly ash with a 60-day compressive strength ranging from 20 to 23 MPa using only NaOH solution with concentrations ranging from 9 to 14 M and curing at low temperatures. For curing, they kept the samples in a controlled chamber at 25-28 °C until mechanical testing. Temuujin et al. (2009) also reported the

development of a geopolymer paste based on fly ash cured at low temperatures, in this case at ambient temperature. They produced a geopolymer with a 28-day compressive strength of 45 MPa from milled fly ash. The alkaline activation of fly ash at low temperatures performed by Somna et al. (2011) and Temuujin et al. (2009) reached relatively good compressive strengths possibly due to an increase of fly ash reactivity by decreasing particle size, their samples were milled down to d_{50} of 10.5 and 6.8 μm , respectively. Production of mortars based on fly ash-based geopolymers has also been widely reported. Atis et al. (2015) prepared a geopolymer mortar with a 1-day compressive strength as high as 120 MPa made with a mixture of sand and fly ash in a ratio of 3:1, activated with NaOH (Na = 14% wt.%) and cured at 115 °C for 24 h. Other high-strength geopolymer mortars were produced with fine class C fly ash ($d_{50}=9 \mu\text{m}$) by Chindaprasirt et al. (2010), who made a geopolymer mortar with a 28-day compressive strength of 86 MPa by an alkaline activation using a mixture of sodium silicate and 10 M sodium hydroxide, in a mass ratio of 1 to 1. Rattanasak et al. (2009) also used a $\text{Na}_2\text{SiO}_3/\text{NaOH}$ mass ratio of 1 but with 15 M sodium hydroxide and produced a geopolymer mortar with a compressive strength of 70 MPa after curing for two days at 65 °C. The same curing conditions were used by Chindaprasirt et al. (2009) who obtained a fly ash based-geopolymer mortar with a 2-day compressive strength of 35 MPa. Provis et al. (2009) did an extensive study varying the liquid/binder ratio and M_s in the total solution and found that the best compressive strength was obtained for M_s values from 1 to 1.5 and a liquid/binder ratio ranging from 0.5 to 0.7.

Table 2.2. Reported mixtures for fly ash-based geopolymer pastes and mortars.

Fly ash type (SiO ₂ /Al ₂ O ₃ , molar ratio)	Alkaline solution	Liquid/binder (weight ratio)	Compressive Strength (MPa) [age]	Curing Conditions	Reference
Class F (2.55)	Na ₂ SiO ₃ + KOH (Ms=1.2)	0.33	59 [5d]	24 h at room temperature + 24 h at 80 °C	(Kong et al., 2007)
Class C (3.40)	Na ₂ SiO ₃ + NaOH (Ms= 1.5, Na ₂ O=10% by weight)	0.40*	63.4 [28d]	8 h at 75 °C + 23 °C for 28 d (using vinyl film)	(Guo et al., 2010)
Class C (3.48)	Na ₂ SiO ₃ + NaOH (Ms= 1.23)	0.30	68.7 [1d]	24 h at 85 °C (sealed container)	(Palomo et al., 1999)
N/A (3.04)	9-14 M NaOH	0.30	20-23 [60d]	At room temperature (Controlled chamber)	(Somna et al., 2011)
N/A (3.71)	Na ₂ SiO ₃ + 14 M NaOH (Si/Al= 2.3, Na/Al= 0.88)	0.25*	45 [28d]	At room temperature	(Temuujin et al., 2009)
Class F (5.38)	NaOH (Na= 14%, weight basis)	0.33*	120 [1d] (with a sand/ash ratio of 3)	24 h at 115 °C	(Atiş et al., 2015)
Class C (3.23)	Na ₂ SiO ₃ + 10 M NaOH (Na ₂ SiO ₃ /NaOH mass ratio = 1)	0.20	86 [28d] (with a sand/ash ratio of 3.23)	1 h of delay time + 3 d at 75 °C	(Chindapasirt et al., 2010)
N/A (3.44)	Na ₂ SiO ₃ + 15 M NaOH (Na ₂ SiO ₃ /NaOH mass ratio = 1)	0.67	70 [2d] (with a sand/ash ratio of 2.75)	48 h at 65°C (cling film)	(Rattanasak et al., 2009)
N/A (3.16)	Na ₂ SiO ₃ + 10 M NaOH (Na ₂ SiO ₃ /NaOH mass ratio = 1.5)	0.67	35 [2d] (with a sand/ash ratio of 2)	48 hr at 65 °C (cling film)	(Chindapasirt et al., 2009)
Class F (2.79)	Na ₂ SiO ₃ + NaOH (Ms= 1-1.5)	0.5-0.7	50 – 60 [3d] (with a ash/ sand ratio of 0.47)	3 d at 40 °C (humid atmosphere)	(J. Provis et al., 2009)

* Water to dry binder weight ratio.

2.3.2. Ground granulated blast furnace slag

Iron slag is a by-product of the manufacturing process of crude iron in blast furnaces. According to Van Oss (2002), iron slag, also known as blast furnace slag (BFS), is generated by the combination of impurities and flux agents removed during the formation of crude iron at high temperatures. The production of BFS per ton of crude iron depends highly on the grade of the iron ore, with a ratio of 1.2 tons of slag per ton of crude iron in low grades ores. BFS is produced in large quantities, the US accounts

for 18 million tons in 2017 according to USGS data (U.S. Geological Survey, 2017). According to Van Oss (2002), there are three main types of BFS that can be formed depending on the cooling process during crude iron production, and each one can be used for a different purpose. Air cooled BFS, cooled at ambient conditions, is mostly used as an aggregate for road metal, concrete and asphalt. Foamed BFS, which is obtained when cooled by a water jet stream, is used for the production of lightweight concrete. And finally, BFS cooled in water, also known as GGBF, is utilized primarily, after a grinding process, as partial substitution of OPC due to its moderate hydraulic cementitious properties. This blended cement develops a low initial strength making its use unsuitable for applications where high initial resistance is needed. However, GGBFS based geopolymers show good mechanical strength even at the initial stage. Chemical composition analysis of GGBFA shows that it is made primarily of CaO, SiO₂ and Al₂O₃ in decreasing amounts (e.g. GGBFS used by Oh et al. (2010) contained 41.78% of CaO, 33.04% of SiO₂ and 13.35% of Al₂O₃).

Table 2.3 presents the optimal mixtures for the GGFBS-based geopolymers and their compressive strengths reported in the scientific literature. Even though some studies have shown that high contents of Ca in raw materials like fly ash diminish the mechanical properties of the resulting geopolymer, GGBFS based geopolymers, which have high amounts of Ca showed great initial and final strengths (up to 50 MPa) when 10 M sodium hydroxide was used as an activator (Oh et al., 2010). The authors suggest that GGBFS and fly ash class C have different chemical forms of calcium. While Ca stays unreacted in class C fly ash reducing the mechanical strength, Ca in GGBFS is able to form C-S-H bonds that seem to increase the final mechanical strength (Oh et al., 2010). In the same direction, Cheng & Chiu (2003) also produced a geopolymer with high compressive strengths from GGBFS activated with sodium silicate and 10 M potassium hydroxide. Schilling et al. (2011) produced GGBFS-based geopolymers with a 28-day compressive strength of 38 MPa which were cured at 23 °C in a saturated atmosphere. There are also studies that report the production of mortars based on alkaline activation of GGBFS, for instance, Omer et al. (2015) presented a GGBFS-based geopolymer mortar with a sand/GGBFS ratio of 2.75, that had a 7-day compressive strength of 47 MPa using an activating solution of sodium silicate and 8M NaOH with a mass ratio of 2.5. Meanwhile, a geopolymer mortar from GGBFS

(sand/GGBFS ratio = 4) was produced by Islam (2014) with a compressive strength of 60 MPa at 3 days after casting.

Table 2.3. Reported mixtures for GGBFS-based geopolymer pastes and mortars.

SiO ₂ /Al ₂ O molar ratio	Alkaline solution	Liquid/binder (weight ratio)	Compressive Strength (MPa) [age]	Curing Conditions	Reference
4.04	Na ₂ SiO ₃ + 10 M KOH (SiO ₂ /Al ₂ O ₃ = 3.36 , SiO ₂ /K ₂ O = 1.32)	N/A	70 [1d]	3 h at 60 °C (sealed moulds)	(Cheng & Chiu, 2003)
4.21	10 M NaOH	0.4	50 [14d]	7 d at 80 °C (water bath)	(Oh et al., 2010)
6.26	5 M NaOH	0.4*	38 [28d]	28 d at 23 °C (>95% RH)	(Schilling et al., 2011)
4.11	Na ₂ SiO ₃ + 8 M NaOH (Na ₂ SiO ₃ /NaOH mass ratio = 2.5)	0.4	47.3 [7d] (sand/GGBFS ratio of 2.75)	24 h at 60 °C (with plastic bags)	(Omer et al., 2015)
4.03	Na ₂ SiO ₃ + 12 M NaOH (Na ₂ SiO ₃ /NaOH mass ratio = 2.5)	0.4	60 [3d] (sand/GGBFS ratio of 4)	24 h at 65 °C (with plastic films)	(Islam et al., 2014)

* Water to dry binder weight ratio.

2.3.3. Construction and demolition waste

The amount of construction and demolition wastes (C&D) is enormous and keeps growing in the world. According to the United States Environmental Protection Agency (EPA), 534 million tons of C&D were generated by the US alone in 2014 (U.S. Environmental Protection Agency, 2016), while in Europe around 970 million were produced in 2006 (Monier et al., 2011). Even though C&D are considered to be harmless materials, it still requires a place for disposal and improper management can cause serious effects on the environment and human health (Marzouk & Azab, 2014). Unfortunately, waste management systems in less developed countries are inefficient and operate either with low or without standards (Wilson et al., 2006), resulting in wastes disposed of in uncontrolled landfills and dumps (Gamarra & Salhofer, 2007). Therefore, recycling C&D to produce new building materials is beneficial, not only from the point of view of the reduction of energy and raw materials, but also to control the decrease of available land for mining resources and for landfills (A. Allahverdi & Najafi, 2009). Moreover, if the amounts of C&D and fly ash produced per year in the

U.S. are used as a reference, the potential and interest should increase in the future towards the former material since its generation is about 10 times larger than fly ash.

i. Clay brick powder

Clay brick powder, a C&D product, has shown great potential as raw material for geopolymer production. Baronio and Binda (1997) claimed that clay brick powder has potential pozzolanic activity due to the destruction of the crystalline network when the hydroxyl groups in clay minerals are lost when subjected to high-temperature conditions during production. Chemical composition of clay brick powder is mainly SiO_2 and Al_2O_3 , however, it also contains important amounts of CaO , Fe_2O_3 and MgO (Allahverdi & Najafi, 2009; Baronio & Binda, 1997; Komnitsas et al., 2015; Rakhimova & Rakhimov, 2015; Reig et al., 2013a; Reig, et al., 2016; Zawrah et al., 2016).

A compilation of research results concerning the formulation of the alkaline activating solution for clay brick powder to produce geopolymer binders and mortars is presented in Table 2.4. Allahverdi et al. (2009) developed a binder with a 28-day compressive strength of 40 MPa by activation of clay brick powder ($\text{SiO}_2=53.4\%$, $\text{Al}_2\text{O}_3=10.5\%$) with an alkaline solution of $M_s = 0.6$ and with a Na_2O content of 8% (by weight of dry binder). In this study, samples were cured at ambient temperature and high relative humidity (95%). They also found that the addition of waste concrete powder to the mixture is detrimental for the compressive strength e.g. a replacement of 40% of brick powder with concrete waste powder caused a decrease in the compressive strength from 40 MPa to 16.5 MPa (A. Allahverdi & Najafi, 2009). On the other hand, Komnitsas et al.(2015) studied the geopolymerization of three types of C&D and found that the best formulation for the alkaline activating solution for their brick powder ($\text{SiO}_2=57.8\%$, $\text{Al}_2\text{O}_3=14.95\%$) was a mixture of Na_2SiO_3 and 8M NaOH and the optimal curing temperature was 90 °C, for 7 days using plastic bags to avoid water evaporation. Furthermore, they demonstrated that the compressive strength of brick powder-based geopolymers increased from 8 up to 35 MPa when particle size was reduced from d_{50} of 35 to 6.6 μm . These results are in agreement with data reported by Pathak et al. (2014), who studied the effect of particle size in the compressive strength of clay brick powder-based geopolymers. They concluded that finer particles of the brick powder obtained by a longer milling process formed geopolymer binders with better compressive strength (Pathak et al., 2014). Pure waste fired clay brick powder

(SiO₂=50.16 %, Al₂O=15.95 %) were activated by Zawrah et al. (2016) using Na₂SiO₃ and 8 M NaOH with a Na₂SiO₃/NaOH volume ratio of 2.5, to produce a paste with a 90-day compressive strength of 15 MPa. This 90-day compressive strength increased up to 83 MPa by replacing 60 % of clay brick powder with GGBFS, maintaining same alkaline and curing conditions. Suitability of clay brick powder and GGBFS blending was also demonstrated by Rakhimova & Rakhimov (2015), who manufactured an alkali-activated paste with a 28-day compressive strength of 120 MPa from a precursor material consisting of 40 % clay brick powder and 60% GGBFS. Similar to this, Reig et al. (2013) produced a geopolymer mortar made of brick powder and sand (sand/brick ratio = 3) by means of mixing the solids with an alkaline solution Na₂SiO₃ and NaOH (Ms= 1.6) reaching a 7-day compressive strength of 41 MPa. A clay brick-based geopolymer mortar was also elaborated by Reig et al. (2013a) with a 7-day compressive strength of 50 MPa mixing sand and brick in a mass ratio of 2 and Ms of 2. Furthermore, there are also reports that focus on blended geopolymers, for example, Reig et al. (2016) studied the influence of the addition of calcium aluminate cement on alkaline-activated mortars based on clay brick powder. They found that a replacement of 40% of clay brick powder by calcium aluminate cement (CAC) could increase the compressive strength of the mortar from 10 to 80 MPa when cured at 20 °C with a RH of 96%.

Table 2.4. Reported mixtures for clay brick powder-based geopolymer pastes and mortars.

SiO ₂ /Al ₂ O molar ratio	Alkaline solution	Liquid/binder (weight ratio)	Compressive Strength (MPa) [age]	Curing Conditions	Reference
8.66	Na ₂ SiO ₃ + NaOH (Ms= 0.6, Na ₂ O= 8% by weight)	0.30*	40 [28d]	At room temperature (humid bath)	(A. Allahverdi & Najafi, 2009)
6.57	Na ₂ SiO ₃ + 8 M NaOH (Na ₂ SiO ₃ =6% , H ₂ O=16%)	0.38	49.5 [7d]	7 d at 90 °C (covered with plastic bags)	(Komnitsas et al., 2015)
5.34	Na ₂ SiO ₃ + 8 M NaOH (Na ₂ SiO ₃ /NaOH volume ratio = 2.5)	0.30	15 [90d]	At room temperature (covered with polythene sheet)	(Zawrah et al., 2016)
5.34	Na ₂ SiO ₃ + 8 M NaOH (Na ₂ SiO ₃ /NaOH volume ratio = 2.5)	0.30	83 [90d] (with GGBFS replacement of 60%)	At room temperature (covered with polythene sheet)	(Zawrah et al., 2016)
4.15	Na ₂ SiO ₃ + NaOH (Ms= 1.5, Na ₂ O= 5% by weight)	N/A	120 [28d] (with GGBFS replacement of 60%)	At room temperature (RH=95 %)	(Rakhimova & Rakhimov, 2015)
5.12	Na ₂ SiO ₃ + NaOH (Ms= 1.6, Na molality = 8)	0.35*	41 [7d] (sand/brick powder ratio of 3)	7 d at 65 °C (controlled bath)	(Reig, et al., 2013)
5.11	Na ₂ SiO ₃ + NaOH (Ms= 2, Na molality = 7)	0.30*	50 [7d] (sand/brick powder ratio of 2)	7 d at 65 °C (controlled bath)	(Reig et al., 2013a)
5.11	Na ₂ SiO ₃ + NaOH (Ms= 1.6)	0.40*	80 [28d] (sand/brick powder ratio of 3 + CAC replacement of 40%)	28 d at 20 °C (RH=96%)	(Reig et al., 2016)

* Water to dry binder weight ratio.

ii. Concrete waste powder

Concrete waste powder (CWP) has a high content of SiO₂ and CaO with a lower presence of Al₂O₃ and Fe₂O₃. Nevertheless, a pure CWP-based geopolymer with a 7-day compressive strength of 13 MPa was reported by Komnitsas et al. (2015). Another study has reported the production of geopolymers based on CWP blended with alumino-silicate materials as is shown in Table 2.5. Vásquez et al. (2016) claimed that CWP needs the addition of a reactive alumina source in order to develop higher mechanical strength materials due to its semi-crystalline nature. These authors showed

that the addition of 10% of metakaolin increased the compressive strength from 25.6 MPa (pure CDW geopolymer) to 46.4 MPa under the same conditions. Ahmari et al. (2012) confirmed this by showing that pure CWP based geopolymers achieved low resistances, while CWP blended with fly ash (in a 1:1 ratio) produced hybrid geopolymers with good mechanical properties. This hybrid geopolymer, activated with NaOH (5-10M) and sodium silicate (sodium silicate/NaOH ratio of 1:2), resulted in even better mechanical properties than pure fly ash geopolymers activated with the same alkaline conditions. Hence, the addition of CWP could improve the mechanical properties of fly ash geopolymers (Ahmari et al., 2012). However, mixing red clay brick powder and CWP for geopolymer production did not show good results as in the case of metakaolin or fly ash blending. This could suggest that there is not enough Al content to form sufficient polysialate units. In this regard, Allahverdi and Kani (2009) have reported that replacing 40% of CWP by red clay brick powder caused a decrease of the compressive strength from 49.5 MPa (pure brick powder-based geopolymer) to 16.5 MPa at 28 days of curing time.

Table 2.5. Reported mixtures for CWP-based geopolymer pastes and mortars.

SiO ₂ /Al ₂ O molar ratio	Alkaline solution	Liquid/binder (weight ratio)	Compressive Strength (MPa) [age]	Curing Conditions	Reference
8.95	Na ₂ SiO ₃ + NaOH (Na ₂ O = 6% , SiO ₂ /Al ₂ O ₃ = 8)	0.22	46.4 [28d] (with metakaolin replacement of 10%)	24 h at 25 °C + curing chamber (covered with polythene sheet)	(Vásquez et al., 2016)
6.63	Na ₂ SiO ₃ + 8 M NaOH (Na ₂ SiO ₃ =6% , H ₂ O=17%)	0.48	13 [7d]	7 d at 90 °C (covered with plastic bags)	(Komnitsas et al., 2015)
3.56	Na ₂ SiO ₃ + NaOH (Na ₂ SiO ₃ /NaOH mass ratio = 2)	0.29*	35 [7d] (with fly ash replacement of 50%)	At room temperature (covered with plastic bag)	(Ahmari et al., 2012)
8.97	Na ₂ SiO ₃ + NaOH (Ms= 0.6, Na ₂ O= 8% by weight)	0.26*	16.5 [28d] (with clay brick replacement of 40%)	At room temperature (humid bath)	(A. Allahverdi & Najafi, 2009)

* Water to dry binder weight ratio.

2.3.4. Mine tailings

Mine tailings (MT) are a residual material from mine operations and are mainly composed of finely-ground sand to silt-sized rock particles, water and processing reagents used to extract valuable minerals from the ore (Natural Resources Canada, 2013). With the number of minerals extracted and processed each year around the world by the mining industry, the volume of MT is enormous, e.g. worldwide MT generation is estimated to be more than 7 billion tons per year. Therefore, this matter should be of concern in metal producer countries since the proper disposal of MT requires not only a lot of lands but can also constitute a hazardous environmental problem as dangerous heavy metals can reach aquatic ecosystems (Salomons, 1995). As MT disposal is potentially toxic in some cases and could involve an elevated cost to satisfy environmental regulations, its potential use as raw material for geopolymerization has generated great interest. Copper and tungsten MT have already been widely studied as starting materials for geopolymer production (see Table 2.6). The chemical composition of copper MT used by Ahmari et al. (Ahmari et al., 2012) was mainly SiO_2 and Al_2O_3 with a substantial presence of CaO and Fe_2O_3 .

On the other hand, Pacheco-Torgal et al. (2009) evaluated the use of tungsten MT that was composed mainly by SiO_2 , Al_2O_3 , Fe_2O_3 and K_2O . They used a mixture of NaOH 24 M and sodium silicate ($M_s = 1.34$) as the activating solution and cured their samples at room temperature, the geopolymers formed showed a 56-day compressive strength of 45.5 MPa. The same curing conditions were employed by Pacheco-Torgal & Jalali (2010) to obtain a tungsten MT geopolymer paste with a 28-day compressive strength of 40 MPa using an alkaline solution with a $\text{Na}_2\text{SiO}_3/\text{NaOH}$ mass ratio of 2.5. On the other hand, Silva et al. (2012) employed a curing process consisting of two stages to produce a binder with a compressive strength up to 24 MPa. In the first stage, specimens were left at room temperature and then were heated at 80 °C in the second stage. Regarding the use of copper MT, Ahmari et al. (2012) studied the effect of curing temperatures and alkaline solutions in the activation and resulting compressive strength of geopolymers. They found that an alkaline solution of sodium aluminate and 10 M NaOH at a mass ratio of 1.25 and a curing temperature of 90 °C for 7 days produced a copper MT-based geopolymer with a compressive strength of 17 MPa. On the other hand, Zhang et al. (2011) produced hybrid geopolymers made from mixtures of fly ash and copper MT, which resulted in a compressive strength of 3 MPa at 7 days of age.

Table 2.6. Reported mixtures for MT-based geopolymer pastes and mortars.

Fly ash type (SiO ₂ /Al ₂ O molar ratio)	Alkaline solution	Liquid/binder (weight ratio)	Compressive Strength (MPa) [age]	Curing Conditions	Reference
Tungsten MT (5.46)	Na ₂ SiO ₃ + NaOH (Ms= 1.34)	1	45.5 [56d]	At room temperature	(Pacheco- Torgal et al., 2009)
Tungsten MT (5.46)	Na ₂ SiO ₃ + NaOH (Na ₂ SiO ₃ /NaOH mass ratio = 2.5)	1	40 [28d]	At room temperature	(Pacheco- Torgal & Jalali, 2010)
Tungsten MT (6.34)	Na ₂ SiO ₃ + NaOH (Na ₂ SiO ₃ /NaOH mass ratio = 4)	0.25	24 [63d]	7 days at 20 °C + 56 days at 80 °C	(Silva et al., 2012)
Cooper MT (15.56)	NaAlO ₂ + 10 M NaOH (NaAlO ₂ / NaOH = 1.25)	0.27*	17 [7d]	7 days at 90 °C (capped mold)	(Ahmari, et al., 2012)
Cooper MT (15.56)	NaOH 15 M	0.27*	3 [7d]	7 days at 60 °C (Plexiglas cap)	(Zhang et al., 2011)

* Water to total dry binder weight ratio.

2.4. Natural fibers as reinforcement for geopolymer binders

2.4.1. Natural fibers

The use of synthetic or man-made fibers such as carbon, glass, aramid and polypropylene to reinforce polymer matrices producing fiber-reinforced composites with improved mechanical properties is widely spread in the automotive, aerospace and construction industries (Lau & Hung, 2017). In construction materials, the application of fiber reinforcement can modify the tensile and flexural strength, and fracture energy of cementitious matrices (Yan & Chouw, 2013). In the fiber-reinforced composites, fibers are not only reinforcement but also the main source of strength while matrix glues all the fibers together in shape and transfers stresses between the reinforcing fibers. At the same time, fibers carry the loads along their longitudinal directions (Chandramohan & Marimuthu., 2011). Comparing to synthetic fibers, natural fibers are more preferred as reinforcements within cementitious composites for decades due to an increasing environmental concern for developing environmentally-friendly and energy efficient materials (Silva et al., 2010; Yan & Chouw, 2013). Natural fibers have several attractive advantages that surpass synthetic fibers: i) low weight, ii) low cost, iii) widely available, iv) biodegradable, v) renewable and non-

hazardous sources, vi) desirable aspect ratio, and vii) good relative tensile and flexural strength (Xie et al., 2010). Natural fibers can be classified by their origin in plant, animal and mineral fibers. According to Lau et al. (Lau & Hung, 2017) plant- and animal-based fibers are suitable for the production of fiber-reinforced polymers. However, animal fibers are less favorable for this application in comparison to plant and synthetic fibers considering that their collection from animals is more difficult to implement on a large scale. Therefore, plant fibers are a better option for production of fiber-reinforced geopolymer composites, since their specific mechanical properties are competitive with synthetic fibers (Yan et al., 2014; Yan et al., 2016). However, there are several important factors, i.e. fibre selection (including type, harvest time, extraction method, aspect ratio, treatment and fibre content), matrix selection, interfacial strength, fibre dispersion, fibre orientation, composite manufacturing process and porosity, that need to be considered (Pickering et al., 2016). All plant fibers are mainly composed of cellulose and lignin (lignocellulose fibers). However, the amount of cellulose varies according to the species and age of the plant. Cellulose is a hydrophilic glucan polymer formed by a linear chain of glucose units linked together through $\beta(1 \rightarrow 4)$ bonds, while lignin is a biochemical material that works for structural support in plants (Mohanty et al., 2005). The degree of polymerization of cellulose is responsible for the mechanical properties of the fiber and varies depending on the species of the plant (Mohanty et al., 2005). The chemical structures of cellulose and lignin are shown in Figure 2.1.

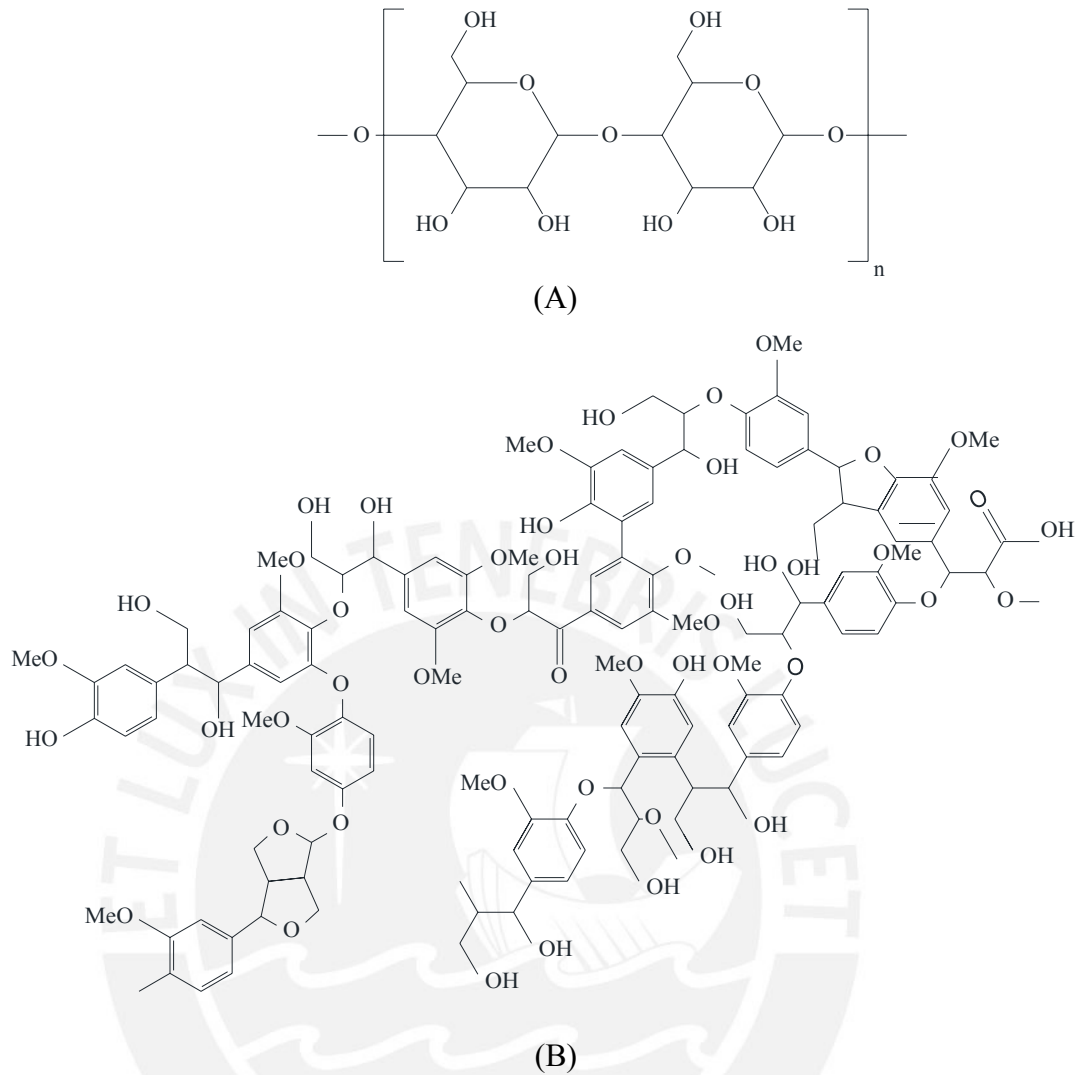


Figure 2.1. Chemical structures of (A) cellulose and (B) lignin.

Plant fibers (lignocellulose fibers) have been used as reinforcing materials for geopolymer matrices for a long time. They are very suitable applications of these fibers in geopolymers since the geopolymerization occurs at high alkaline condition and lignocellulose fibers have strong resistance to a high level of alkaline condition. Plant fibers have three main categories depending on the part of the plant from which they extracted (Jawaid & Abdul, 2011): i) Bast or stem fibers (jute, flax, hemp, ramie, kenaf, etc.), ii) Leaf fibers (sisal, banana, manila hemp, pineapple (PALF), etc.), and iii) Seed fibers (cotton, coir, oil palm, etc.)

A diagram with a classification according to their origin or botanical type is shown in Figure 2.2 (Jawaid & Abdul, 2011; Yan et al., 2016).

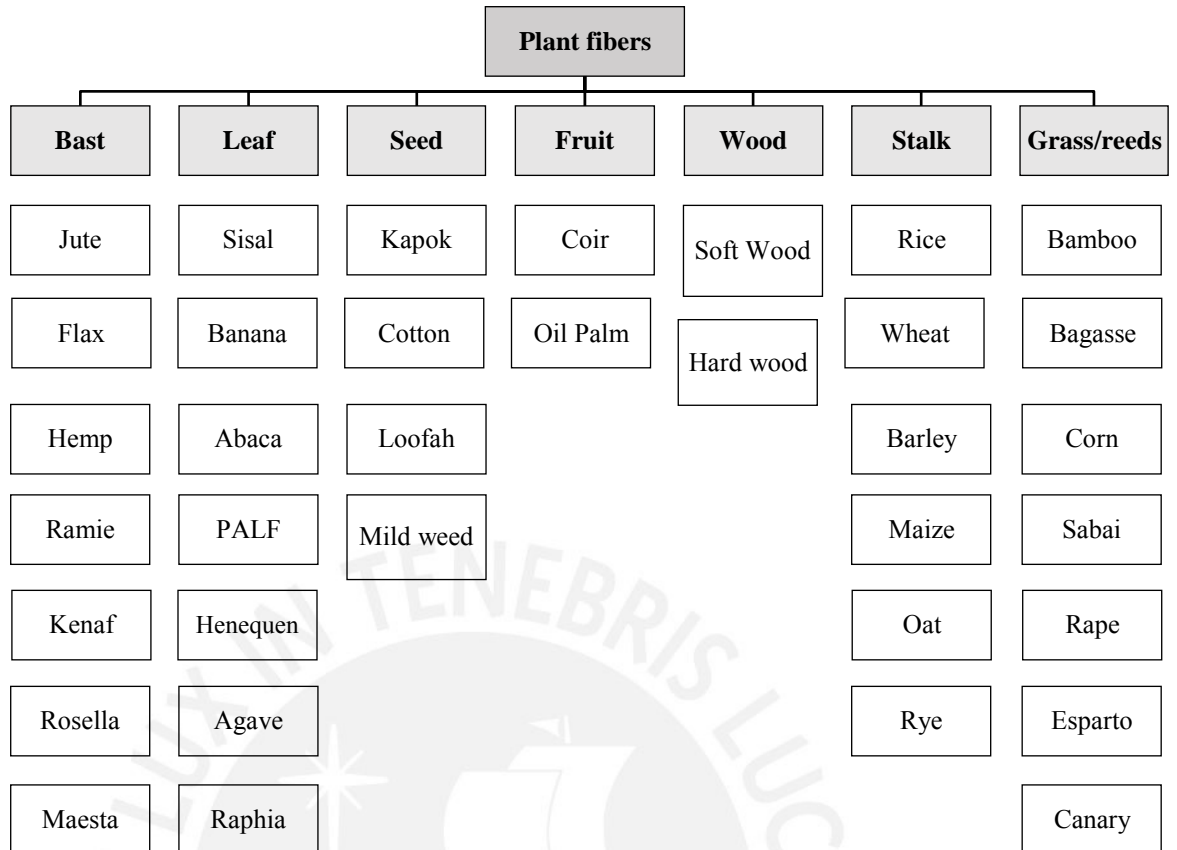


Figure 2.2. Classification of natural plant fibers (adapted and modified from Yan et al. (2016) and Pickering et al. (2016)).

The mechanical properties of plant fibers depend on fiber diameter and length, moisture gain and microfibril angle, etc. The tensile strength of cellulose fibers decreases with an increase of fiber length since the longer fibers have possibly more defects and thus could fail prematurely compared to a shorter fiber (Yan et al., 2016). Cellulosic plant fibers have high moisture absorption capacity and poor dimensional stability because they usually swell in contact with water. Moreover, when natural fibers are used as reinforcement, adhesion between fibers and matrix can be affected by the hydrophobicity/hydrophilicity of fibers in relation to the matrix. The presence of pendant hydroxyl and polar groups in the components can lead to high moisture uptake, poor fiber and matrix adhesion causing a low mechanical performance of the composite (Yan et al., 2016). There are several efforts to improve the fiber and matrix adhesion to obtain better durability of components: i) Hornification (Ardanuy et al., 2015): Fibers undergo drying and rewetting cycles; ii) Mercerization (Yan, 2012): Alkaline pre-treatment of fiber; and iii) Silane treatment (Pradeep & Rakesh, 2012): Improvement of water resistance.

2.4.2. Plant fibers reinforcement for geopolymer matrices

The number of published papers focusing on the use of natural plant fibers to enhance mechanical properties of geopolymer matrices has increased in recent years (Yan et al., 2016), however, it is still limited compared to the number of studies conducted with conventional cementitious materials. Review articles elaborated by Pacheco-Torgal et al. (2011) and Hejazi et al. (2012) have shown that natural fiber reinforcement of conventional building materials as OPC-based products and soil is a topic that has gained great attention. There are a few papers that present the state of the art of fiber reinforced geopolymer composites (Sakulich, 2011; Shaikh, 2013), but, they only focus on man-made or synthetic fibers and fabrics such as geopolymer matrices reinforced with steel fibers (Zhao et al., 2007), carbon fibers, glass fibers (Natali, Manzi, & Bignozzi, 2011), polypropylene fibers (Puertas et al., 2003), polyvinyl alcohol fibers (Sun & Wu, 2008; Yunsheng et al., 2008), basalt fibers (Dias & Thaumaturgo, 2005; W. Li & Xu, 2009) as well as carbon fabrics (Lin et al., 2008), basal fabrics (Waltraud et al., 2003) and glass fabrics (Pernica et al., 2010). Therefore, this section will focus on presenting research done with plant natural fibers as reinforcement in two forms: randomly oriented short natural fibers and non-woven and woven fibers (layers).

i. Applications of short plant fibers randomly oriented

Short random fiber reinforcement of geopolymer matrices are of special interest for large-scale applications as building materials since they do not require advanced processing techniques, traditional mixing machines can be used. A list of available literature regarding short natural fiber reinforcement of geopolymer composites is given in Table 2.7. Correia et al. (2013) studied the reinforcement of metakaolin-based geopolymers with sisal fibers and pineapple leaf fiber (PALF). Sisal fibers were extracted from the leaves of the *Agave sisalana*, while PALF were obtained from *Ananas conusus* plant. 25 mm-long fibers were used in 3% ratio (by volume) with the geopolymer matrix. Even though the compressive strength of MT-based geopolymers reinforced with sisal fibers and PALF decreased compared to unreinforced geopolymers, the traction and impact performance of the resulting composites significantly improved for both fibers. For PALF reinforced geopolymers, the flexural, tensile and impact strength increased by 100%, 111% and 200%, respectively, in relation to the unreinforced matrix. While for the sisal fiber, the reinforced MT-based

geopolymer showed an increase of 43%, 100% and 113% in its flexural, tensile and impact strengths, respectively. A similar behavior was reported by Chen et al. (2014) using alkali-treated sweet sorghum fiber to reinforce fly ash based geopolymers activated with 10 M sodium hydroxide with a liquid/solid ratio of 0.36. These researchers performed the alkaline pre-treatment of the fibers to improve adhesion and cohesion between matrix and fibers (Alomayri et al., 2013a; Chen et al., 2014). Chen et al. (2014) performed unconfined compression, splitting tensile and flexural tests in order to determine the optimum content of fibers and found it to be 2% (by weight) of fiber with respect to fly ash. As reported by Correia et al. (2013), they also observed that the presence of fibers induced a little loss of compression strength in all specimens. Nevertheless, the main function of fiber reinforcement is to provide ductility and control of cracking and not to enhance compressive strength (Bentur & Mindess, 2006). Sá et al. (2016) explored the use of micro and short bamboo fibers to reinforce metakaolin-based geopolymers. Their research also evaluated the influence of water and alkali pre-treatment of the fibers in the mechanical properties of the resulting geopolymer composite. Compression tests results indicate again that the addition of water and alkali-treated bamboo fibers caused an important loss of compressive strength. However, the flexural strength significantly increased from 4.50 (control matrix) to 24.95 MPa when alkali bamboo micro fibers and strips (5 wt%) were used to reinforce the geopolymer matrix. Korniejenko et al. (2016) have also reported a wide variety of plant fibers to reinforce fly-ash based geopolymers, they have worked with 1% (by weight of the composite) of fiber content. They used cotton fibers (30 mm length), sisal fibers (3 mm length), raffia fibers (3 mm length), and coir fiber (3 mm length). Unconfined compressive test and three-point bending tests showed that the addition of cotton, sisal and coir caused a slight improvement of the mechanical properties after 28 days of curing. However, the addition of raffia fibers proved not to be compatible with fly ash-based geopolymers and resulted in a decrease of both compressive and flexural strengths. Similar to this, Alomayri et al. (2013) evaluated different cotton fiber contents to reinforce fly-ash based geopolymers also. They used an alkaline solution to solid ratio of 0.35 and found that a cotton fiber content of 0.5% (by weight) produced the highest flexural strength, flexural modulus, and fracture toughness. They observed an adequate fiber dispersion and good interaction between the matrix and the fibers with this fiber content. More fiber, as

also mentioned by Chen et al. (2014), resulted in lower mechanical properties due to the formation of voids and fiber agglomeration.

Even though there are no reports of studies on the effect of the fiber length with short natural fiber reinforcement of geopolymers, it is an important aspect that will need to be evaluated. It is known that, in general, fiber length plays an important role in the final strength achieved by composites, and in geopolymer composites in particular, Lin et al. (2008) have reported that 7 mm carbon fibers gave the highest flexural strength in geopolymers compared to carbon fiber lengths of 2 and 12 mm.

Table 2.7. Reported studies regarding plant short-fiber reinforced geopolymer composites.

Natural fiber	Geopolymer type	Fiber content by weight (%)	Compressive Strength (MPa)		Flexural Strength (MPa)		Tensile Strength (MPa)		Reference
			Without fibers	With fibers	Without fibers	With fibers	Without fibers	With fibers	
Sisal	Metakaolin	3*	6.9	6	1.4	2.8	0.45	0.95	(Correia et al., 2013)
Pineapple leaf	Metakaolin	3*	6.9	3.3	1.4	2.0	0.45	0.90	(Correia et al., 2013)
Alkali-treated sweet sorghum	Fly ash (Class F)	2	27.7	22.9	3.6	5	2.5	3.4	(Chen et al., 2014)
Bamboo fibers and strips	Metakaolin	5	55.7	29.7	4.50	24.95	N/A	N/A	(Sá et al., 2016)
Cotton	Fly ash (Class F)	1	24.78	28.42	5.55	5.85	N/A	N/A	(Korniejenko et al., 2016)
Sisal	Fly ash (Class F)	1	24.78	25.16	5.55	5.90	N/A	N/A	(Korniejenko et al., 2016)
Raffia	Fly ash (Class F)	1	24.78	13.66	5.55	3.05	N/A	N/A	(Korniejenko et al., 2016)
Coir	Fly ash (Class F)	1	24.78	31.36	5.55	5.25	N/A	N/A	(Korniejenko et al., 2016)
Cotton	Fly ash (Class F)	0.5	N/A	N/A	10.4	11.7	N/A	N/A	(Alomayri et al., 2013a)

* Fiber content by volume of the composite

ii. Applications of plant fiber layers

Plant fibers reinforcement with non-woven and woven layers with alternated fiber orientation have been studied to produce fiber reinforced geopolymer panels (see Table 2.8). Use of non-woven plant fibers layers to reinforce geopolymer matrix has been reported by Alzeer & MacKenzie (2013), who reinforced geopolymers based on halloysite with flax fibers. Their fabrication process consisted of alternating layers of

geopolymer resin and unidirectional stripped flax fiber bundles. The best reinforcement was achieved with 10% (by weight) of fibers, which showed an impressive increase in flexural strength from 5.8 MPa to 70 MPa. On the other hand, Kriven et al. (2013) employed quasi-aligned and random corn husk fiber bundles to produce composite panels. Their results showed that, although both flexural and impact strengths decreased in the reinforced panels, a significant improvement in deformation resistance was gained with the addition of fiber bundles. There are also reports regarding woven plant fibers, best known as fabric-reinforced composites. For instance, Alomayri et al. (2013b) produced a reinforced class F fly ash geopolymer composite with cotton fabrics. In this study, the authors evaluated the flexural and impact strengths and fracture toughness with two (1.4 wt %) up to six (4.1 wt %) layers of pre-dried fabric. The results showed that all three mechanical properties increased with the presence of the fabric, with a 2.1 % fiber content the optimum, which corresponds to 3 layers. The loss of mechanical performance with more layers was suggested to be caused by a lower fiber-matrix interfacial bonding. However, in a more recent study, Alomayri et al. (2014b) solved this limitation by wetting the fabric with the geopolymer paste and applied a 25 kg load for 3 hours on the composite. This fabrication method produced geopolymer composites with up to 40 (with an 8.3 wt %) fabric layers that showed significantly better mechanical properties (31.7 MPa flexural strength and 15.6 MPa impact strength). The same procedure was used by Assaedi et al. (2015) with flax fabrics and fly ash based-geopolymers obtaining a compressive strength of 91 MPa and a flexural strength of 23 MPa. It is important to highlight that mechanical performance of these fabric-reinforced geopolymer composites depend on the orientation of the fabrics with respect to the applied load, as it was demonstrated by Alomayri et al. (2014a). They reported that the mechanical properties in the parallel direction of the fabrics are lower than those in the perpendicular direction. They suggested that loads applied perpendicularly in respect to the cotton fabrics they used resulted in detachment and delamination of the composite.

Table 2.8. Reported studies regarding plant fabric reinforced geopolymer composites.

Natural fiber	Geopolymer type	Fiber content by weight (%)	Compressive Strength (MPa)		Flexural Strength (MPa)		Impact Strength (kJ/m ²)		Reference
			Without fibers	With fibers	Without fibers	With fibers	Without fibers	With fibers	
Flax bundles	Dehydroxylated halloysite	10	N/A	N/A	5.8	70	N/A	N/A	(Alzeer & Mackenzie, 2013)
Corn husk bundles	Metakaolin	5	N/A	N/A	14.1	8.8	N/A	N/A	(Kriven et al., 2013)
Cotton fabric	Fly ash (Class F)	2.1	N/A	N/A	8.2	~ 12.5	2.1	~ 6.8	(Alomayri et al., 2013b)
Cotton fabric (perpendicular to fabrics)	Fly ash (Class F)	8.3	21.0	~ 90.0	8.2	31.7	2.1	15.6	(Alomayri et al., 2014b, 2014a)
Cotton fabric (parallel to fabrics)	Fly ash (Class F)	8.3	21.0	~ 60.0	8.2	~ 26.0	N/A	N/A	(Alomayri et al., 2014a)
Flax fabric	Fly ash (Class F)	4.1	19.4	91	4.5	23	N/A	N/A	(Assaedi et al., 2015)

2.4.3. Other natural fibers

Table 2.9 summarizes published research focusing on the usage of protein-based fibers as reinforcement of geopolymer composites. Alzeer and MacKenzie (2012) studied metakaolin-based geopolymers activated with NaOH and sodium silicate and reinforced with two types of wool fibers at 5 wt% of the content. They used merino and carpet wool fibers in three different conditions: without any cleaning and treatment, cleaned and treated. They reported that the addition of bundles of wool fibers could increase the flexural strength of geopolymer matrices and that cleaning and treatment of fibers had an effect in the mechanical properties of the reinforced composite.

Table 2.9. Reported studies regarding other natural fibers reinforced geopolymer composites.

Natural fiber	Raw material	Content (%)	Compressive Strength (MPa)		Flexural Strength (MPa)		Tensile Strength (MPa)		Reference
			Without fibers	With fibers	Without fibers	With fibers	Without fibers	With fibers	
Cleaned merino wool	Metakaolin	5	N/A	N/A	5.8	9.1	N/A	N/A	(Alzeer & MacKenzie, 2012)
Treated carpet wool	Metakaolin	5	N/A	N/A	5.8	8.7	N/A	N/A	(Alzeer & MacKenzie, 2012)

CHAPTER 3: Analysis of the production conditions of geopolymer matrices from construction and demolition wastes

Abstract. The improvement of the mechanical properties of geopolymer matrices relies on the characteristics of the source material as well as in a proper optimization of the alkaline activating solution and curing conditions during geopolymerization. Since geopolymer production parameters need to be determined for each source material, this study presents the analysis of the conditions for obtaining high compression strength matrices from Fired Clay Brick Powder (FCBP). The applied optimization methodology analyzed the influence of the formulation of the activators and curing conditions by changing the sodium oxide (Na_2O) content, the $\text{SiO}_2/\text{Na}_2\text{O}$ molar ratio, the water/binder ratio, the oven curing temperature and oven curing time. The results of the uniaxial compression tests of over 70 samples indicated that the compression strength is directly affected by these parameters. The tests allowed defining the optimum conditions of the FCBP-based geopolymer formulations and curing conditions that resulted in high compression strengths of up to 37 MPa. The methodology for the optimization of production conditions of geopolymer matrices validated in this study demonstrated to provide consistent results and, therefore, could be applied for the analysis of the production process of geopolymers based on other aluminosilicate sources.

3.1. Introduction

Generation of construction and demolitions wastes (C&D) is reaching enormous amounts around the world. For example, the US alone generated 534 millions of tons of C&D in 2014 (EPA, 2016), the European Union (EU) produces approximately 855 million tons per year (which represents the 33.3 % of the total wastes in EU), while it is estimated that C&D production in China is around 600 million tons per year (Ghosh & Ghosh, 2015). Fired clay brick constitutes one of the major components of C&D, representing an average of 30% of total C&D in the EU (Böhmer et al., 2008) and reaching higher amounts (up to 54%) in some countries such as Spain (Ministerio de Fomento de España, 2010). Considering these large amounts of C&D produced per year, it is an urgent necessity to evaluate potential uses for these waste materials. In

this respect, recycling C&D components, such as fired clay brick, to develop alternative building materials has environmental and economic advantages since it reuses wastes and therefore avoids filling scarce landfills and also diminishes extraction and production of new raw materials (Nehdi & Khan, 2004). Green cements

that use fired clay brick wastes have been developed by partial replacement of Ordinary Portland Cement (OPC) (Ay & Ünal, 2000; F. Pacheco-Torgal & Jalali, 2010b; Puertas et al., 2010). Up to 35% of fired clay brick powder (FCBP) has been incorporated in OPC with similar performance (Ay & Ünal, 2000). Other studies have reported the use of crushed fired clay brick as coarse and fine aggregates in concrete production with no loss of mechanical strengths compared to conventional concretes.

Given that the use of cement is still necessary to produce construction materials with high mechanical properties even though its preparation generates an equal amount of CO₂ per ton produced, it is beneficial to find alternatives to replace OPC. Therefore, a greener approach to produce a cementitious material with low CO₂ emissions could be based on geopolymers made from alumino-silicate wastes or industrial by-products. However, to spread their use, these new eco-friendly construction alternatives need to have similar mechanical properties to the traditional ones (Joseph Davidovits, 1994).

FCBP has shown great potential as raw materials for geopolymer production (Allahverdi & Najafi, 2009; Komnitsas et al., 2015; Rakhimova & Rakhimov, 2015; Reig et al., 2013a; Reig et al., 2013; Reig et al., 2016; Zawrah et al., 2016). Baronio and Binda (1997) have claimed that FCBP has pozzolanic activity potential due to the destruction of the crystalline network when structural hydroxyl groups of clay minerals

are lost with high temperatures during production. The optimal alkaline activation of geopolymers varies widely depending on the type of raw material due to differences on particle size distribution, morphology, mineralogical and chemical composition. Reig et al. (2013a; 2013), Komnitsas (2015) and Allahverdhi et al. (2009) optimized the formation of FCBP -based geopolymers by varying the alkaline solution parameters such as the silica modulus (M_s), the sodium oxide content (Na_2O) or NaOH concentration, and also the water/binder ratio. On the other hand, the curing conditions showed to have a direct and significant influence on the mechanical properties of the geopolymers produced as in (Atiş et al., 2015; Djobo et al., 2016). The objective of this research is to optimize the alkaline activating solution composition and the curing conditions to produce high strength geopolymers from FCBP from the construction industry.

3.2. Materials and Experimental plan

3.2.1. Description of the raw materials

Fine powders of commercial fired clay bricks from the construction industry in Lima were obtained after a milling process consisting of three phases. First, the entire brick was placed in an impact crusher to obtain pieces smaller than 25 mm. After that, a rolling mill reduced the particle size to 0.5 mm or less, which were finally placed in a ball mill for 4 hours. A particle size analyzer, SediGraph 5100, was used to determine the particle size distribution envelope of FCBP (Figure 3.1a) using the sedimentation method where the particle mass is measured directly via X-ray absorption. FCBP exhibited a mean particle size of 19.66 μm , d_{90} of 58.66 μm , d_{50} of 7.39 μm and d_{10} of 1.21 μm (Figure 3.1a). The micromorphology of FCBP was investigated by scanning electron microscopy (SEM), using a Thermo Fisher Scientific Quanta 250 microscope. As shown in Figure 3.1b, FCBP presented a very irregular and crystal-like shape (in contrast to the spherical shape of fly ash (Duxson & Provis, 2008)).

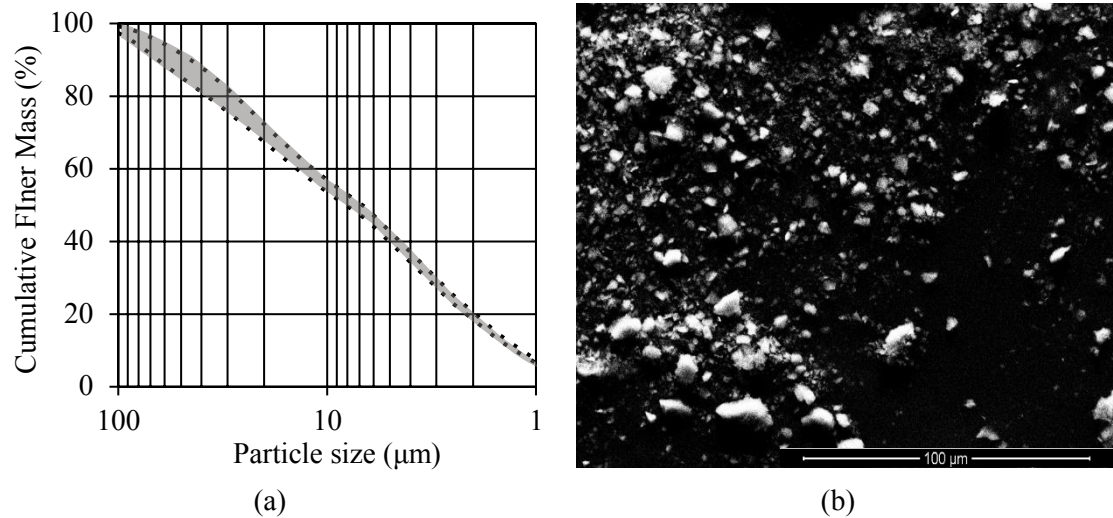


Figure 3.1. Particle size distribution and morphology of FCBP: (a) Granulometric curves envelope of grinded raw material and (b) SEM micrograph.

The chemical composition of the raw material was obtained by X-ray fluorescence spectroscopy (see Table 3.10) using an ARL OPTIM'X Spectrometer. As shown, FCBP can be used as a good source material for the development of geopolymers due to their high content of SiO_2 (53.45 %) and Al_2O_3 (20.52 %) (J. Davidovits, 1989). The quantitative analysis of elemental composition (%) of FCBP performed by SEM equipped with an energy dispersive X-ray (EDX) confirmed the results from X-ray fluorescence spectroscopy.

Table 3.10. Chemical composition of FCBP by X-ray fluorescence spectroscopy.

Raw material	Oxide content (% wt.)							
	SiO_2	Al_2O_3	Fe_2O_3	K_2O	MgO	CaO	Na_2O	Others
FCBP	53.45	20.52	7.80	2.63	1.85	1.62	1.50	10.63

In order to gather the mineralogical composition of the FCBP, X-ray diffraction (XRD) analysis was performed using a Bruker D8 Discover DAVINCI XRD instrument equipped with a Lynxeye detector and a $\text{Cu K}\alpha$ X-ray tube. The XRD data were collected for phase angles (2θ) between 10° and 70° , with a 0.02° step and an integration time of 4 seconds. Crystalline phases were identified from PDF-2 database (2013 edition) using Bruker AXS Software Diffrac.EVA 4. According to the X-ray diffractogram shown in Figure 3.2, FCBP contains mainly quartz, SiO_2 , a mixture of feldspars, $(\text{Na, Ca, K})\text{AlSi}_3\text{O}_8$, and hematite (iron oxide), as well as other lesser minerals such as goethite, $\text{FeO}(\text{OH})$ and actinolite, $\text{Ca}_2(\text{Mg}_{4.5-2.5}\text{Fe}_{0.5-2.5})\text{Si}_8\text{O}_{22}(\text{OH})_2$.

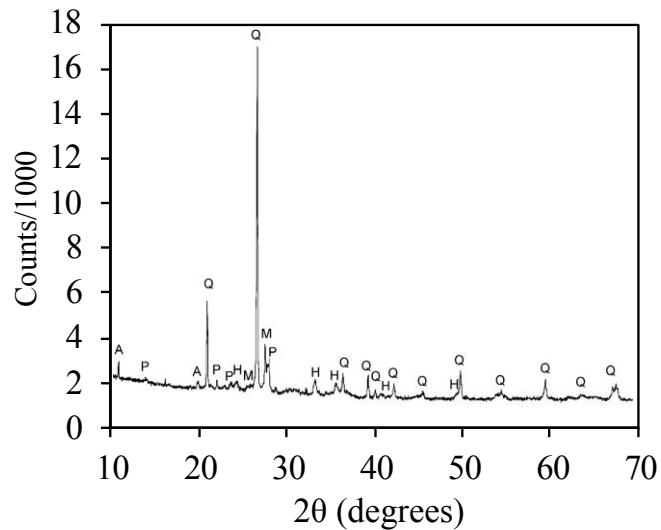


Figure 3.2. X-ray diffractograms of FCBP. Q: Quartz (SiO_2); H: Hematite (Fe_2O_3); P: Plagioclase (albite/anortite, $(\text{Ca}, \text{Na})\text{Al}_2\text{Si}_2\text{O}_8$); A: Actinolite ($\text{Ca}_2(\text{Mg}_{4.5-2.5}\text{Fe}_{0.5-2.5})\text{Si}_8\text{O}_{22}(\text{OH})_2$); M: Microcline ($\text{KAl}_2\text{Si}_2\text{O}_8$); C: Calcite (CaCO_3); K: Orthoclase/Microcline ($\text{KAl}_2\text{Si}_2\text{O}_8$).

3.2.2. Characterization of geopolymer matrices

Mechanical and chemical characterization of geopolymer matrices were conducted after 7 days of fabrication. For performing the mechanical characterization, the uniaxial compressive strength of FCBP-based geopolymers was studied following the guidelines of ASTM C109/C109M – 16a (ASTM, 2016). Silicon moulds (Figure 3.3b) were employed to produce 50 mm cubic samples (Figure 3.3c), which were used for the mechanical characterization. An electromechanical testing machine MTS model Exceed 45.105 controlled by displacement was used for all compression tests (Figure 3.3a). The displacement rate of the load frame was set to 0.5 mm/min. Load cell displacements were recorded in all tests and were taken as global deformations. For physical characterization, density was calculated to evaluate the influence of all studied variables on the geopolymer samples.

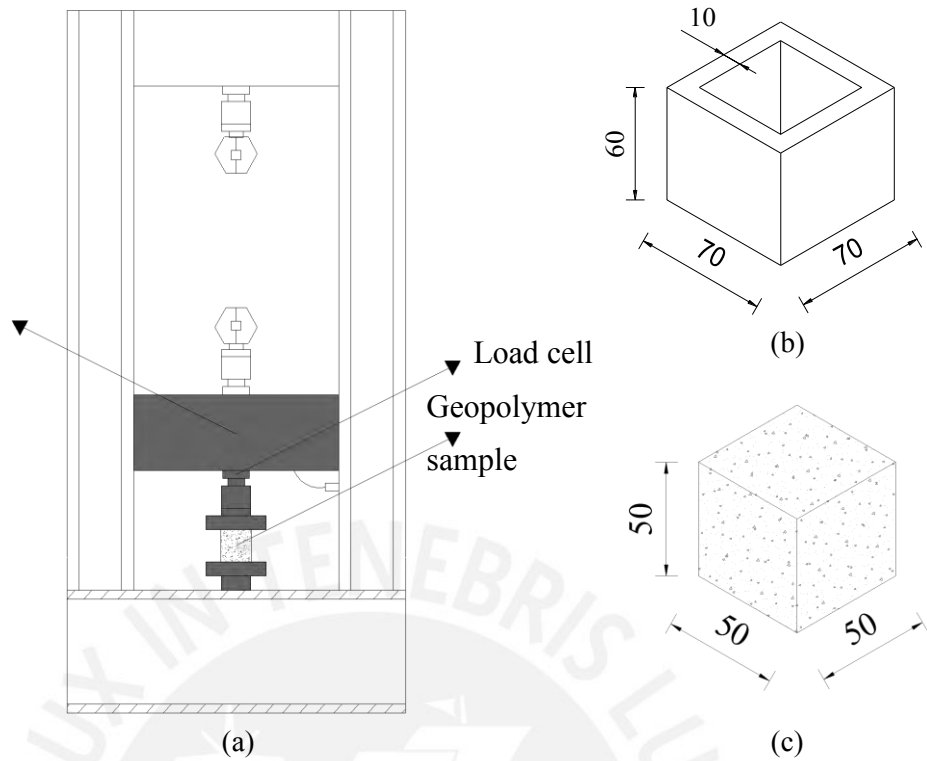


Figure 3.3. Mechanical characterization of geopolymer matrices to uniaxial compression: (a) Schematic view of the compression test; (b) Schematic view of the silicon molds and (c) Resulting geopolymer cubic sample. (units in mm)

For chemical characterization, Fourier-transform infrared spectroscopy (FT-IR) was used by means of a Perkin Elmer model 100 FT-IR spectrometer. Samples were prepared as thin transparent pellets using KBr, while spectra were recorded in transmittance mode with 32 scans. IR spectra were obtained in order to follow the change in bonding and chemical environments around Al and Si atoms present in geopolymers made from FCBP. The bands observed in the spectra are those commonly found in geopolymers and their precursors (Catauro et al. 2015; Lee & Van Deventer, 2003), and they have been compiled in Table 3.2. Wavenumbers between 1250 and 400 cm^{-1} are associated with vibrations of covalent bonds between oxygen and Si and Al atoms. As geopolymer formation involves both dissolution and polymerization reactions bonds must be broken and formed during the process. It is also expected that the chemical environment around the Si and Al atoms change as oxygen atoms create new bridges between them, which should be reflected in their vibration bands.

Table 3.11. IR bands and their corresponding bond vibration present in FCBP-based geopolymers (Catauro et al. 2015; Lee & Van Deventer, 2003).

Wavenumber (cm ⁻¹)	Bond vibration
950 – 1250 (strong)	Asymmetric stretching (Si-O-Si and Al-O-Si)
1165 (shoulder)	Asymmetric stretching (Si-O-Si)
1115 – 1140 (shoulder)	Asymmetric stretching (Si-O-Si and Al-O-Si)
1077 (strong)	Asymmetric stretching (Si-O-Si and Al-O-Si)
950 – 980 (shoulder)	Si-O stretching (Si-O-R*)
882 (strong)	Si-O stretching and OH bending (Si-OH)
798 (medium)	Symmetric stretching (Si-O-Si)
727 (shoulder)	Symmetric stretching (Si-O-Si and Al-O-Si)
620 (shoulder)	Symmetric stretching (Si-O-Si and Al-O-Si)
561 (strong)	Symmetric stretching (Al-O-Si)
466 (strong)	Bending (Si-O-Si and O-Si-O)

*R= Na or K

3.2.3. Preparation of samples

Alkaline solutions were prepared by mixing sodium hydroxide pearls (99.27 % purity, New China Chemicals Co., Ltd.), sodium silicate solution (28% SiO₂ + 8% Na₂O + 64% H₂O, Abastecimientos Químicos Ciatex S.A.C) and distilled water. Then, the raw material (Figure 3.4a) and the alkaline solution were mixed in a mortar-mixing machine type STJBJ-5 (Zhejiang Tugong Instrument Co., Ltd.) for about 90 seconds after which a homogeneous paste was obtained (Figure 3.4b). Geopolymer matrices were then placed into the cubic silicon molds and samples were subjected to mechanical vibration to remove trapped air bubbles. Afterwards, specimens (Figure 3.4c) were cured in an oven at different temperatures and curing times. The curing process was completed when the samples were left at ambient temperature (~ 20°C) until mechanically tested (all samples were de-molded after the first day of curing and were tested after 7 days of production).



Figure 3.4. Production process of geopolymers: (a) FCBP; (b) FCBP geopolymer paste; (c) FCBP-based geopolymer cubic sample.

Five variables were defined as key parameters in the alkaline activation: silica modulus (M_s), Na_2O content, water/binder ratio (w/b), curing temperature and curing time. M_s is defined as the molar ratio between SiO_2 and Na_2O in the alkaline solution while the variable defined as Na_2O (wt. %) is the content of sodium oxide in the alkaline solution used in the geopolymer matrix. A four-stage experimental research plan was designed taking into count these variables to optimize the alkaline activating solution composition and the curing conditions for geopolymers production. Table 3.12 shows all twenty-six series of geopolymer matrices considered in this study (three specimens were tested to uniaxial compression in each series). The first stage was related to optimize the M_s . In the second stage, the objective was to determine the best Na_2O content. The effect of water content was investigated in the third stage by means of the weight ratio between water (including the water in the sodium silicate solution) and the dry raw material. Finally, the fourth stage involved the study of the effect of the curing temperature and curing time on the development of mechanical resistance of FCBP-based geopolymer matrix.

Table 3.12. Experimental plan for the optimization of FBCP-based geopolymers production.

Stage	N°	Raw Material	M _s (mol/mol)	Na ₂ O (wt. %)	Water/binder (wt./wt.)	Oven curing temperature (°C)	Oven curing time (days)	Total curing time (days)
I Analysis of the effects of silica modulus (M _s)	1		0.50					
	2		0.75					
	3	FCBP	1.00	8	0.30	65	1	7
	4		1.25					
	5		1.50					
II Analysis of the effects of Na ₂ O content and optimization of the value of silica modulus (M _s)	6			6				
	7		0.50	8	0.29	65	7	7
	8			10				
	9			6				
	10	FCBP	0.55	8	0.29	65	7	7
	11			10				
	12			6				
	13		0.60	8	0.29	65	7	7
14			10					
III Optimization of water/binder ratio	15				0.28			
	16	FCBP	0.60	8	0.27	65	7	7
	17				0.26			
	18				0.25			
IV Optimization of oven curing conditions	19						1	
	20		0.6	8	0.27	65	3	7
	21						1	
	22	FCBP	0.6	8	0.27	80	3	7
	23						7	
	24						1	
	25		0.6	8	0.27	95	3	7
26						7		

3.3. Results and discussion

3.3.1. Analysis of the effects of silica modulus (M_s)

Several authors have demonstrated the importance of defining of an adequate M_s in the production of various types of geopolymers (Reig et al., 2013a; Yadollahi et al., 2015). The existence of an optimum M_s is related to a SiO₂/Na₂O molar ratio appropriated to form a highly crosslinked aluminosilicate network, which reduces the presence of unreacted silica (Provis et al., 2012).

The influence of silica modulus (M_s) on the 7th-day compressive strength was assessed keeping constant all the remaining variables. In this first stage, the Na₂O content, water/binder ratio, oven curing temperature and oven curing time were fixed at 8%, 0.30, 65°C and 1 day.

Density values for all samples of FCBP were around 2.0, regardless of the M_s indicating that density is not affected by the SiO₂/Na₂O molar ratio (see Figure 3.5a).

On the other hand, Figure 3.5b show the 7th-day compressive strength results of FCBP-based geopolymers for M_s ratios of 0.50, 0.75, 1.00, 1.25 and 1.50. The results

indicate an inverse relationship of the compressive strength and the value of M_s for FCBP-based geopolymers. The 7th-day compressive strength increased from 0.6 to 1.9 MPa when M_s was reduced from 1.50 to 0.50 (Figure 3.5b).

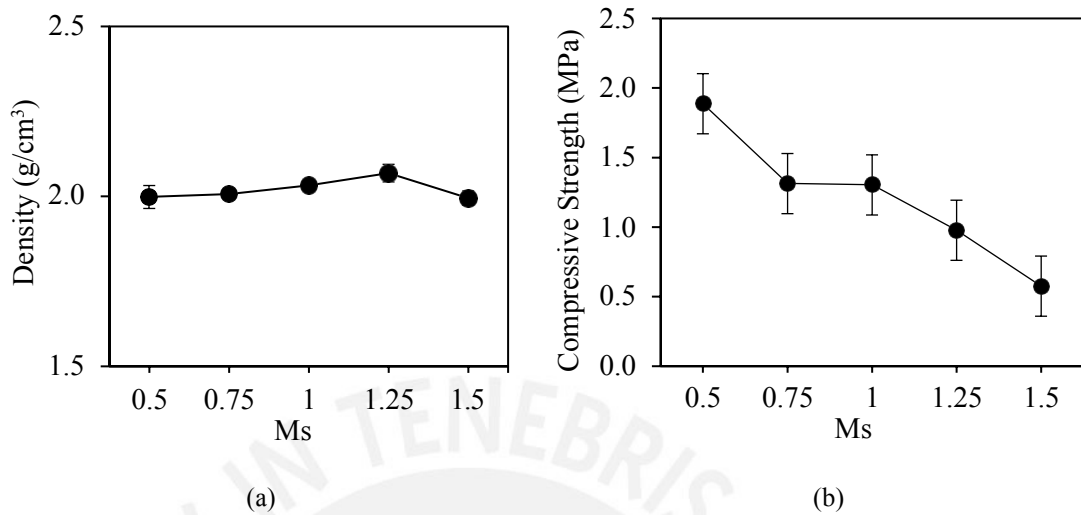


Figure 3.5. Effect of silica modulus (M_s): (a) Density and (b) 7th-day compressive strength.

The results indicate that the optimum M_s values for FCBP-based geopolymers are around 0.50. Therefore, a more accurate evaluation of this parameter in a smaller range was further carried out for the final definition of the optimum M_s value.

3.3.2. Analysis of the effects of the Na_2O content and optimization of the silica modulus (M_s)

Several authors have found that there is an optimum value of Na_2O content for FCBP-based geopolymers. According to Komnitsas et al. (2015) and Allahverdi & Najafi (2009) the optimum value for the FCBP ones is 8%. According to these works, the optimum Na_2O concentration for geopolymer formation is the one that is able to balance electrical charges in the Si and Al tetrahedral chemical structures, accelerates the geopolymerization reaction and gives higher compressive strengths (Allahverdi et al., 2008; Barbosa, 1999). It is to note that higher Na_2O content might result in the presence of unreacted alkali which usually lowers the mechanical properties, as observed in FCBP-based geopolymers (Komnitsas et al., 2015).

To evaluate the effects of the Na_2O content in the geopolymer matrix production and to determine the optimum value of M_s , density and 7th-day compressive strength were evaluated in samples with different mixtures and oven conditions. The water/binder ratio and the oven curing time were kept constant at 0.29 and 7 days, respectively. The oven curing temperature was 65°C. FCBP-based geopolymer

samples were produced with M_s values of 0.50, 0.55 and 0.60 (all around 0.50 as reported in the previous section) and different Na_2O contents (6, 8 and 10%).

The density results indicate that for a constant Na_2O , the density of geopolymers remained almost constant, regardless of the M_s value. However, for a constant M_s and varying conditions of Na_2O , the density increase significantly with a higher Na_2O content. For instance, density values of 1.71, 1.91 and 2.03 g/cm^3 were obtained in FCBP-based geopolymers for a Na_2O content of 6%, 8% and 10% with a M_s of 0.60, respectively (Figure 3.6a).

The setting time was next analyzed considering varying conditions of Na_2O content. For FCBP-based geopolymers, the setting time was reduced when Na_2O content rises. Such is the influence of the Na_2O content in the setting time that FCBP-based geopolymer mixtures with a $\text{Na}_2\text{O} = 12\%$ were not possible to fabricate because they set too rapidly (in less than one minute). This relationship between Na_2O content and setting time has also been reported by Yadollahi et al. (2015) for pumice based-geopolymers.

Figure 3.6b illustrate the influence of the Na_2O content for a given M_s on the 7th-day compressive strength of FCBP-based geopolymers. As shown, a Na_2O content of 8% gave the highest compressive strength for all M_s values. In the case of FCBP-based geopolymers, the highest compressive strength (21.3 MPa) was obtained when Na_2O content raised from 6% to 8% with a M_s value of 0.60. Nevertheless, when the geopolymer matrix was prepared with a Na_2O content of 10%, the compressive strength was reduced to 7.3 MPa.

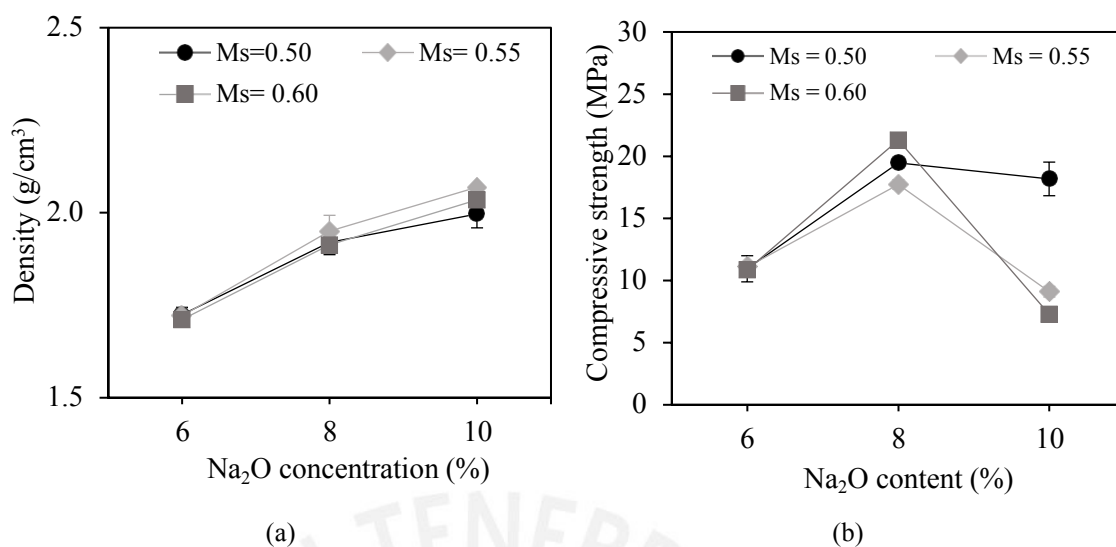
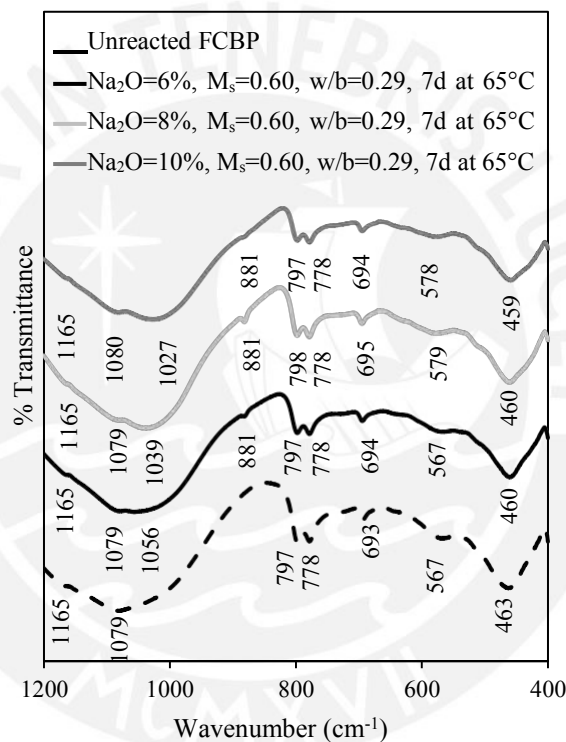


Figure 3.6. Effect of Na₂O content for a given Ms: (a) Density and (b) 7th-day compressive strength.

Figure 3.7 shows the FTIR spectra of unreacted FCBP and FCBP-based geopolymers with different Na₂O contents. Even though the spectra of the geopolymers produced are very similar to the one for unreacted FCBP, some changes can be noticed. The band around 1079 cm⁻¹ in the FCBP spectrum corresponds to T–O–Si asymmetric stretching (where T can be Al or Si) in the unreacted material. Some of these bonds are broken (during depolymerization and dissolution) and some new ones form (during polymerization and gelation) during geopolymer formation. In the initial stages of the reaction, the alkaline activating solution induces depolymerization, which involves the breaking of some of these bonds and the formation of ionic species or moieties with non-bridging oxygen atoms. It has been reported that for low Al content materials, higher concentrations of metal hydroxides are required (Rees et al., 2007). During polymerization, new T–O–Si bonds are formed. This has been explained by Lee and van Deventer (2003) when studying the geopolymerization of heterogeneous amorphous aluminosilicates. They also stated that bands at 1203, 1167 and 1117 cm⁻¹ correspond to satellites of the band at 1079 cm⁻¹. These researchers explained that during the geopolymerization reactions, the shift of the band at 1079 cm⁻¹ to lower wavenumbers is due to the redistribution of the different T–O–Si structures, and presumably increase in Al proportion producing weaker bonds. These changes are apparent in Figure 3.7 with the reduction of the transmission band at 1079 cm⁻¹ and the appearance of bands at 1056, 1039 and 1027 cm⁻¹, with increased Na₂O. Depolymerization increases with more Na₂O since it favors the breakage of T–O–Si

bonds and the formation of ionic species with non-bridging oxygen atoms, including AlO_4^- anions with their corresponding Na^+ counterions.

The lack of sharpness in the bands has been attributed to disorder in the chemical structure, which is expected as geopolymers are mostly amorphous materials (Zhang et al., 2008). This is also supported by the gradual disappearance of the shoulder observed at 567 cm^{-1} in the raw material, which corresponds to Si–O and Al–O bonds present in glasses with certain long-range structural order, such as rings, tetrahedral or octahedral structures (Lee & Van Deventer, 2003), that are destroyed during the polymerization.



(a)

Figure 3.7. FT-IR spectra of unreacted FCBP and FCBP- based geopolymers with different Na_2O contents.

As a conclusion from the second stage of the experimental plan, the optimum alkaline solution for FCBP was determined to have a Na_2O content of 8% with an M_s of 0.60, this produced the highest compressive strength of 21.29 MPa after 7 days of oven curing time.

3.3.3. Optimization of water/binder ratio

Several authors reported the importance of the water content for the production of various types of geopolymers (Allahverdi et al., 2008; Lampris et al., 2009; Reig et al., 2013a; Reig et al., 2013; Yadollahi et al., 2015). Indeed, Reig et al. (2013a) found that the water content was a key parameter for achieving high compressive strengths. Allahverdi et al. (2008) has suggested that when the water content decreases, the total volume of pores and the formation of shrinkage cracks during drying also decrease, resulting in a geopolymer matrix with enhanced mechanical properties. However, lower water contents than the optimum caused a decreased in the compressive strength probably due to the presence of unreacted particles and poor cohesiveness if there is not enough liquid phase to wet all the particles.

In this third stage of the experimental plan, the influence of the water content on the 7th day compressive strength of FCPB-based geopolymer matrices was evaluated. The water content, here named as water/binder ratio, is expressed as the weight ratio between water in the alkaline sodium silicate solution and the dry raw material used in the mixture. Oven curing conditions were kept constant in this stage (65 °C for 7 days).

For FCBP-based geopolymers, Na₂O content and M_s were fixed to 8% and 0.60, respectively. Water/binder ratio was reduced from 0.29 (used in stage 2) until 0.25 with steps of 0.01. Lower values of water content than the lowest ones studied were discarded because of poor workability of the mixtures.

Density measurements after 7 days of curing led to the conclusion that there is no significant change when the water content varies for a constant M_s ratio and Na₂O content (Figure 3.8a).

On the contrary, as shown Figure 3.8b, the water content did exhibit a significant influence in the compressive strength of FCBP-based geopolymers. The highest compressive strength achieved in this second stage for FCBP-based geopolymers (see Figure 3.8b) was 35.2 MPa when the water/binder ratio was 0.27. The results evidenced also the existence of an optimum content of water since values lower than 0.27 (lower amount of water) exhibited low compressive strengths.

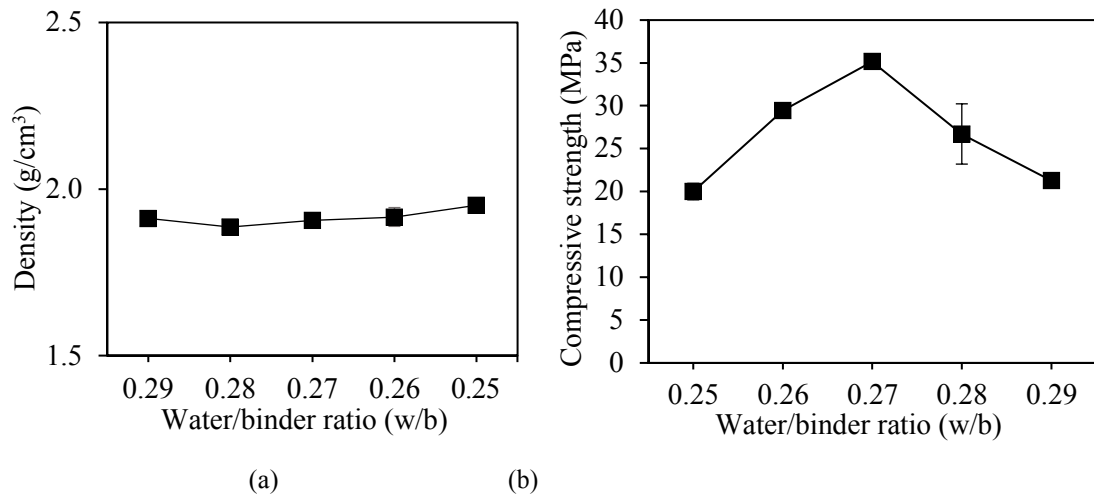


Figure 3.8. Effect of the water/binder ratio: (a) Density and (b) 7th-day compressive strength.

These results indicate that the optimum water/binder ratio depends on the raw material. In addition, the formation of cracks due to shrinkage during drying was strongly reduced when optimum values of water content were employed for FCBP-based geopolymer matrix. From this stage of the experimental plan, it can be concluded that an optimum alkaline activation for FBCP-based geopolymers occurs with an 8% Na₂O content, a 0.60 M_s ratio and a water/binder ratio of 0.27.

3.3.4. Optimization of oven curing conditions

Finally, oven curing conditions were investigated in terms of temperature and curing time using the optimized alkaline solutions found in the previous stages for each geopolymer matrix. These two conditions, curing temperature and curing time, affect some of the processes that occur during geopolymerization: diffusion and reaction rates (favored by higher temperatures) and water evaporation (that comes not only from the activating solution but is also produced during the reactions). Therefore, a balance between these two conditions must be achieved in order to allow the formation of an extended network.

The studied oven curing times for FCBP-based geopolymers were 1, 3 and 7 days while the curing temperatures were 65°C, 80 °C and 95 °C. As expected, for a given temperature, the density decreased with longer oven curing time. A similar behavior in density was observed when the temperature increased for a fixed curing time. For instance, density values of FCBP-based geopolymer samples oven-cured for 7 days were 1.91, 1.83 and 1.74 g/cm³ when the curing temperature was 65°C, 80°C and 95°C, respectively (see Figure 3.9a) The reduction of density could be attributed to the

greater loss of water by evaporation with increasing temperature and longer oven curing times.

The influence of the curing conditions on the 7th-day compressive strength of FCBP-based geopolymers is illustrated in Figure 3.9b. As shown, the results of FCBP-based geopolymer samples cured at 65°C and 80°C are very similar and evidence a linear relationship of compressive strength and the oven curing time. At 95°C, however, there is an important change in behavior for times longer than 3 days: no improvement of compressive strength is observed. These results suggest that, at 95°C, polymerization reactions stop after 3 days probably as a result of a rapid loss of the liquid phase due to higher water evaporation. This affects negatively the geopolymerization since reactive species cannot react if there is no diffusion in the mixture (Komnitsas et al., 2015). For lower temperatures, it is clear that longer curing times result in higher compressive strengths which reach nearly 37 MPa for 7 days.

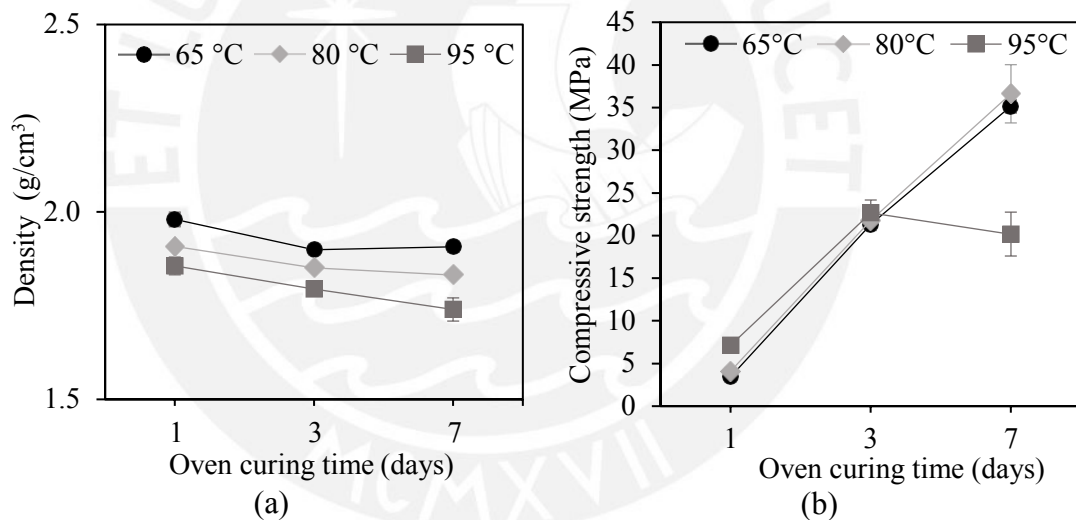


Figure 3.9. Effect of oven curing time on the 7th-day compressive strength for a given oven curing temperature: (a) Density; (b) 7th-day compressive strength.

Failure modes was further studied to understand the influence of different oven curing conditions. As shown in Figure 3.10, failure modes shifts from ductile to a very brittle when oven curing time is increased in FCBP-based geopolymer. Moreover, samples with longer curing times evidenced a higher modulus of elasticity. As shown, an abrupt loss of resistance after reaching peak stress is exhibited in samples cured in an oven for 7 days (this is a typical behavior of brittle cementitious materials). It seems that, unlike fly ash-based geopolymers, FBCP-based geopolymers need more time to react and, therefore, to develop higher mechanical properties. This result is in accordance with other studies of geopolymer samples formed with FCBP as the source

material, that were also cured for 7 days in the oven to produce high strength geopolymer matrices and mortars (Komnitsas et al., 2015; Reig et al., 2013a; Reig et al., 2013).

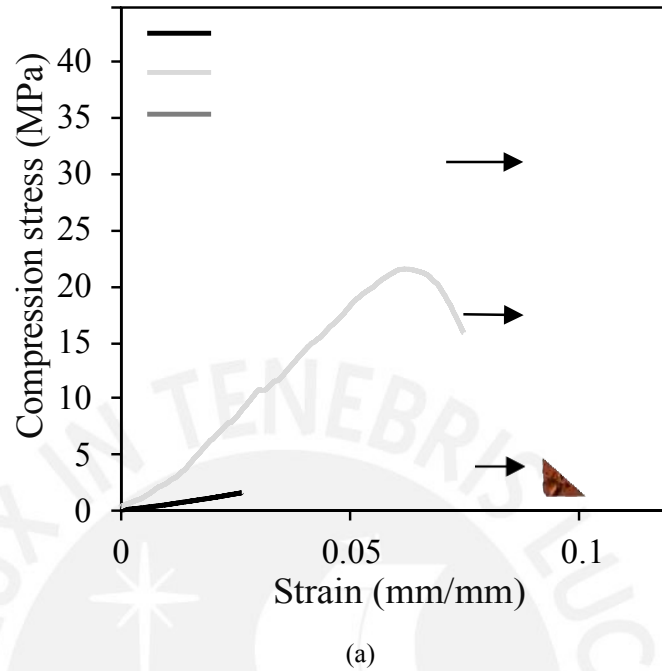


Figure 3.10. Compression stress vs. strain curves and failure modes for a given oven curing time of FCBP-based geopolymers.

Figure 3.11 shows the FTIR spectra of the FCBP and FCBP geopolymers with different oven curing times. Figure 3.11 presents the reduction of the band at 1079 cm^{-1} and the increase of the band at 1031 cm^{-1} , which shows that curing time at 80°C affects also the distribution of the T–O–Si bonds in the products. The shoulder at around 570 cm^{-1} shows a loss of long range order structures after geopolymerization according to previous studies (Panagiotopoulou et al., 2016). From deconvolution analysis of IR spectra of fly ash geopolymers, Lee and van Deventer (2003) assigned a band at $1102\text{--}1105\text{ cm}^{-1}$ to tetrahedral SiO_4 structures, as a prove of polymerization. In the spectra shown in Figure 3.11, a subtle shoulder can be seen around this region, which is more noticeable in the sample cured in the oven for 7 days.

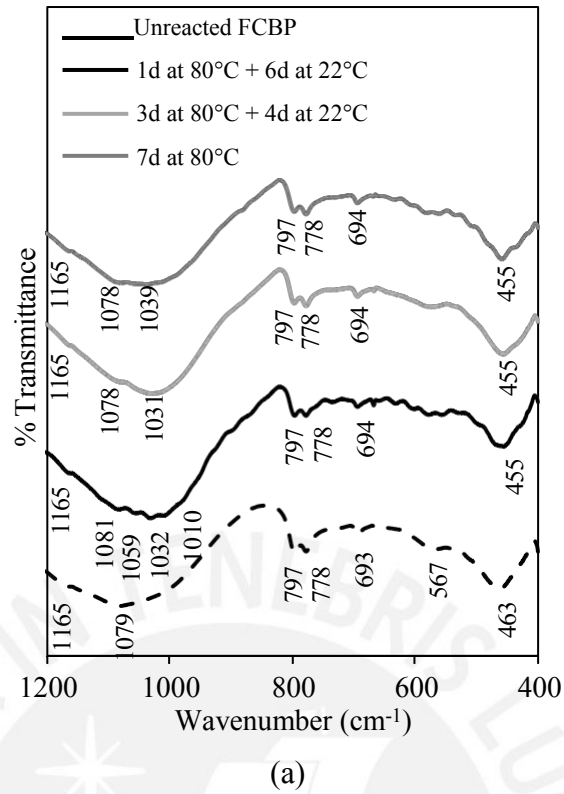


Figure 3.11. FT-IR spectra of unreacted FCBP and FCBP-based geopolymers cured for different oven curing time periods.

As a conclusion from the fourth stage of the experimental plan, an oven curing at 65°C and 80°C for 7 days were defined as the best curing conditions to produce high strength FCBP-based geopolymers, achieving a 7th-day compressive strength around 35 MPa.

CHAPTER 4: Natural cellulose fibers to improve the mechanical behavior of fired clay brick-based geopolymer composites

Abstract. Geopolymer technology has allowed the development of eco-friendly construction materials with high mechanical properties using industrial wastes and residues. However, geopolymers present a fragile behavior and low ductility similar to Portland cement-based materials. This article is focused on the evaluation of jute and sisal fibers as reinforcement of a geopolymer matrix produced from Fired Clay Brick Powder (FCBP). Control samples with no fibers and reinforced matrices with different contents of jute (0.5%, 1.0%, 1.5% and 2.0%) and sisal fibers (0.5%, 1.0%, 1.5%, 2.0%, 2.5% and 3.0%) were produced to study the effect of the fiber content and type on the mechanical properties of the resulting geopolymer composites. Mechanical characterization consisted on compression, splitting tensile and three-point bending tests. The results of compression and splitting tensile tests show the existence of an optimum fiber content that depends on the fiber type while three-point bending tests results indicate a linear relationship between the flexural strength and the fiber content. Presence of sisal fibers increased the compressive, splitting tensile and flexural strength to up to 76%, 112% and 360%, respectively. On the other hand, jute fiber reinforcement caused an increase to up to 64%, 45% and 329% in the compressive, splitting tensile and flexural strength, respectively. Moreover, jute and sisal fiber addition at the optimum content lead to a shift in the failure mode, from a brittle to a more ductile failure, in all mechanical tests.

4.1. Introduction

Several authors have reported the production of geopolymer matrices from waste residues and industrial by-products (i.e. fly ash, ground granulated furnace slag, mine tailings and construction and demolition wastes, among others) which have comparable or even higher mechanical properties with respect to Portland cement-based materials. For instance, Atis et al. (2015) developed a geopolymer mortar made from fly ash that reached a compressive strength of up to 120 MPa after only 1 day of production. In another study, Cheng and Chiu (2003) produced a geopolymer matrix with a 1st-day compressive strength of 70 MPa using ground granulated furnace slag. Pacheco-Torgal and Jalili (2010a) reported the production of tungsten mine tailing-based geopolymers with a 28th-day compressive strength of 40 MPa. High strength geopolymers were also produced with non-metallic minerals such as metakaolin (Bing-hui et al., 2014) and taftan pozzolan (Allahverdi et al., 2008), reaching 28th and 7th-day compressive strengths of 63 MPa and 98 MPa, respectively. In addition to the great compressive strength achieved by geopolymers, this new material also exhibits improved resistance to fire, sulfates and acids (Singh et al., 2015). However, as other cementitious materials, geopolymer matrices present low tensile strengths and exhibit a brittle behavior (Sun & Wu, 2008).

Natural and synthetic fibers reinforcement have been proposed as an option to enhance the performance of geopolymers under tensile stresses. According to Arisoy (2002), the random addition of short fibers to a cementitious matrix increases the toughness by providing energy absorption mechanisms (fiber de-bonding and pull-out), increase ductility by allowing multi-cracking and may increase the strength of the composite by transferring stresses across cracks. Up to now, most of the research regarding fiber reinforced geopolymers has been performed with synthetic fibers such as steel fibers (Zhao et al., 2007), carbon fibers, glass fibers (Natali et al., 2011), polypropylene fibers (Puertas et al., 2003), polyvinyl alcohol fibers (Sun & Wu, 2008; Yunsheng et al., 2008) and basalt fibers (Dias & Thaumaturgo, 2005; Li & Xu, 2009). The reinforcement of geopolymer matrices with natural fibers is receiving more attention in the recent years due to an increasing environmental concern for finding new low CO₂ and energy efficient materials (F. Silva et al., 2010; Yan & Chouw, 2013). For instance, Correia et al. (2013) explored the use of sisal and pineapple leaf fibers at 3% (by volume) of the composite to reinforce metakaolin-based geopolymers. Although

they found that the presence of fibers had a negative influence on the compressive strength, the splitting tensile and flexural strengths were significantly improved when compared to the unreinforced matrix. Sisal fibers improved the flexural and splitting tensile strength by 100% and 111%, respectively, while pineapple leaf fibers increased them by 43% and 100%, respectively, in comparison to the strengths of the unreinforced matrix. Sá et al. (2016) also improved the mechanical properties of metakaolin-based geopolymers by using natural fibers. In their study, water and alkali-treated bamboo fibers and strips (5 %, by weight) were added to the mixture resulting in a composite with enhanced flexural strength (up to 454 % higher than the control sample). However, similarly to the results obtained by Correia et al. (2013) (particularly for pineapple leaf fibers), the compressive strength decreased by about half due to the presence of fibers when compared to the control matrix. On the other hand, Chen et al. (2014), Korniejenko et al. (2016). and Alomayri et al. (2013a) have published research works with natural fiber reinforcement in fly ash-based geopolymer composites. Korniejenko et al. (2016) explored the use of cotton, sisal, raffia and coir fibers at 1% (by weight) by evaluating the compressive and flexural strengths of the resulting composites. Their results show that coir, sisal and cotton fibers increased the compressive strength. Coir fibers produced the highest increase of 27% with respect to the unreinforced matrix. On the contrary, raffia fibers addition resulted in geopolymer composites with a compressive strength 45% lower compared to the unreinforced matrix. In addition, the flexural strength was not influenced by the presence of coir, sisal and cotton fibers, however, the presence of raffia fibers lead also to a decrease in the flexural strength (45% lower). Chen et al. (2014) evaluated the effect of the content of alkali treated sweet sorghum fibers (0, 1, 2 and 3%, by weight) on the mechanical properties of fly ash-based geopolymers. They found an optimum fiber content of 2% (by weight) that caused the highest splitting tensile and flexural strengths (up to 39% and 36% higher, respectively, with respect to the control matrix). However, they also observed a loss in the compressive strength in the resulting geopolymer composites when the fiber content was increased. Alomayri et al. (2013a) also determined an optimum fiber content (0.5 %, by weight) that maximized the flexural strength, flexural modulus and fracture toughness of fly ash-based geopolymer composites.

As it was shown, studies of natural fiber reinforcement in geopolymer composites has been mainly focused in metakaolin and fly ash-based geopolymers. However, high

compressive strengths have also been achieved in geopolymer matrices produced with fired clay brick powder (FCBP) as shown by Allahverdi et al. (2009), Komnitsas et al. (2015), Zawrah et al. (2016), Rakhimova and Rakhimov (2015) and Reig et al. (2013b; 2013; 2016). For instance, Komnitsas et al. (2015) reported the production of FCBP-based geopolymer matrices with a 7th-day compressive strength up to 49.5 MPa, while Rakhimova and Rakhimov (2015) produced a hybrid geopolymer mortar with a 28th-day compressive strength of 120 MPa. From an environmental point of view, FCBP is a perfect candidate as a raw material for the development of an eco-friendly building composite considering the large amounts of fired clay brick wastes produced around the world. For instance, the European Union alone produces around 855 million tons per year of construction and demolition wastes (Ghosh & Ghosh, 2015), an average of 30% of this is estimated to be fired clay brick residues (Böhmer et al., 2008). Therefore, a natural fiber reinforced FCBP-based geopolymer composite is an excellent option to replace traditional building materials, not only because of its low CO₂ emission, but also for it utilizes wastes from this industry. Consequently, the objective of this study is to evaluate common natural cellulose fibers (sisal and jute) as reinforcement to improve the mechanical properties of FCBP-based geopolymers.

4.2. Materials and Experimental plan

4.2.1. Materials

Jute fibers are extracted from *Corchorus capsularis* and *Corchorus olitorius*, while sisal fibers are obtained from *Agave sisalana*. Both natural fibers are mainly composed by cellulose, hemicellulose and lignin but in different proportions. Jute and sisal fibers were selected for the present study since they are considered as future fibers by the Food and Agriculture Organization of the United Nations (FAO) due to the benefits they cause to the environment (Food and Agriculture Organization of the United Nations (FAO), 2010). It is estimated that a hectare of jute plants consumes about 15 tonnes of carbon dioxide (CO₂) and releases 11 tons of oxygen (FAO, 2010). On the other hand, sisal crops absorb more CO₂ than they produced, and the organic wastes produced during sisal fiber production could be employed in industries such as bioenergy generation, animal feed and fertilizer production (FAO, 2010). From the literature, jute fibers are chemically composed by 58-63% of cellulose, 20-24% of hemicellulose, and 12-15% of lignin (by weight) (Li et al., 2006), while sisal fibers contain 43-56% of cellulose, 21-24% of hemicellulose and 7-9% of lignin (by weight)

(Pan et al., 1999). The average diameter of the jute and sisal fibers were 53 and 137 μm , respectively, which were determined using a Mitutoyo dial thickness gauge (model 7301). Both fibers were obtained from commercial products (ropes) and cut to a length of 10 mm, approximately, and were added to the geopolymer matrix during the production process with no pre-treatment. Figure 4.12 shows micrographs of (a) jute and (b) sisal fibers.

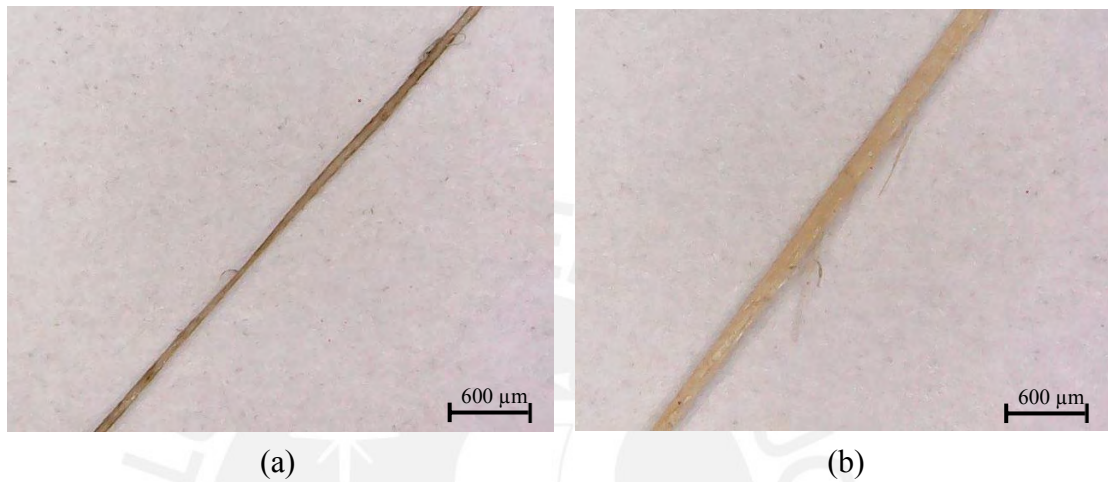


Figure 4.12. Natural fibers used as reinforcement of FCBP-based geopolymer matrix: (a) Jute fiber and (b) Sisal fiber.

Milled fired clay bricks from construction wastes in Lima (Peru) were used as source material for the production of the geopolymer composites. Milling process consisted of three phases: brick particles passed through i) an impact crusher, ii) a rolling mill, and iii) a ball mill. Particle size distribution analysis of FCBP resulted in a mean particle size of 17.14 μm (Figure 4.13a). The SEM micrograph shown in Figure 4.13b show a very irregular and crystal-like shape morphology for FCBP.

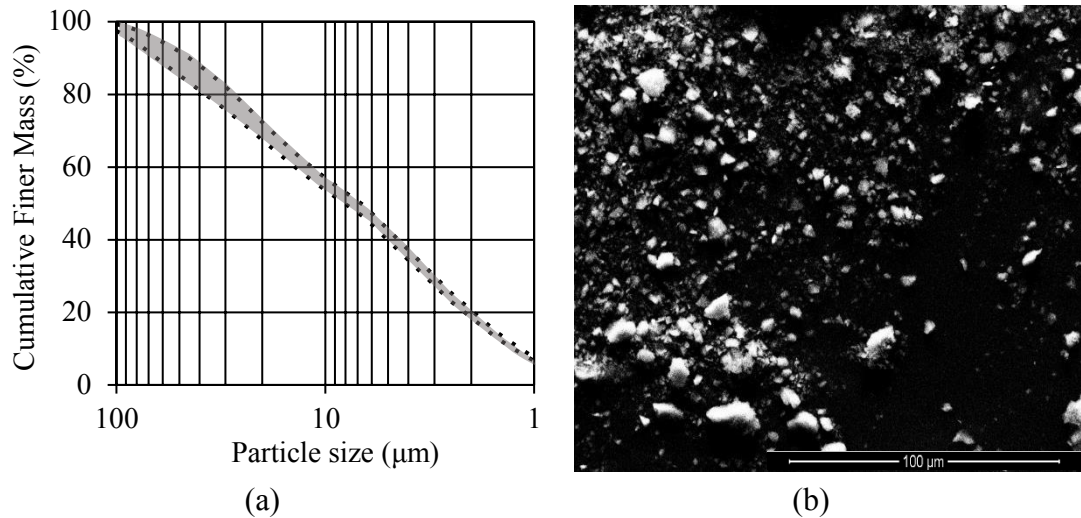


Figure 4.13. Particle size distribution and morphology of FCBP: (a) Granulometric curves envelope and (b) SEM micrograph.

X-ray fluorescence analysis of the FCBP showed a chemical composition (see Table 4.1) with high content (by weight) of SiO_2 (53.45%), Al_2O_3 (20.52%) and Fe_2O_3 (7.80%). More information regarding chemical, physical and microscopy details of the FCBP used in this work can be found in (Silva et al., 2019).

Table 4.13. Chemical composition of FCBP by X-ray fluorescence spectroscopy.

Oxide content (w/w, %)							
SiO_2	Al_2O_3	Fe_2O_3	K_2O	MgO	CaO	Na_2O	Others
53.45	20.52	7.80	2.63	1.85	1.62	1.50	10.63

Alkaline activation solution was prepared by mixing NaOH pearls (99%, purity), sodium silicate solution and distilled water. The chemical composition of the sodium silicate was SiO_2 28%, Na_2O 8%, and H_2O 64% by weight.

4.2.2. Research procedures

First, tensile strengths of jute and sisal fibers were investigated by means of direct tensile tests carried out in a MTS Exceed 42.503 machine with 5 kN capacity at a displacement rate of 6 mm/min (see Figure 4.14a). Single fiber tensile tests were performed following the guidelines of ASTM D3822 (ASTM, 2001). To evaluate the influence of the addition of jute and sisal fibers in the mechanical properties of FCBP-based geopolymer composites, uniaxial compression tests (Figure 4.14d), splitting tests (Figure 4.14f), and three-point bending tests (see Figure 4.14h) were performed according to procedures described in ASTM C109 (ASTM, 2016), ASTM C496

(ASTM, 2017) and ASTM 348 (ASTM, 1998), respectively. 50 mm-side cubic samples were used for compression tests (see Figure 4.14c). Cylindrical specimens (40 mm diameter and 80 mm height) were used for splitting tests, while three-point bending tests involved prismatic samples with approximate dimensions of 40 mm x 40 mm (cross section) x 160 mm (length) (Figure 4.14e and Figure 4.14g, respectively). An electromechanical testing machine MTS Exceed 45.105 (Figure 4.14b) with 100 kN capacity was used for all mechanical tests of geopolymer composites. The displacement rate of the load frame was set to 0.5 mm/min for all tests, and the global displacements corresponding to the displacements of the load frame were recorded for all the mechanical tests.

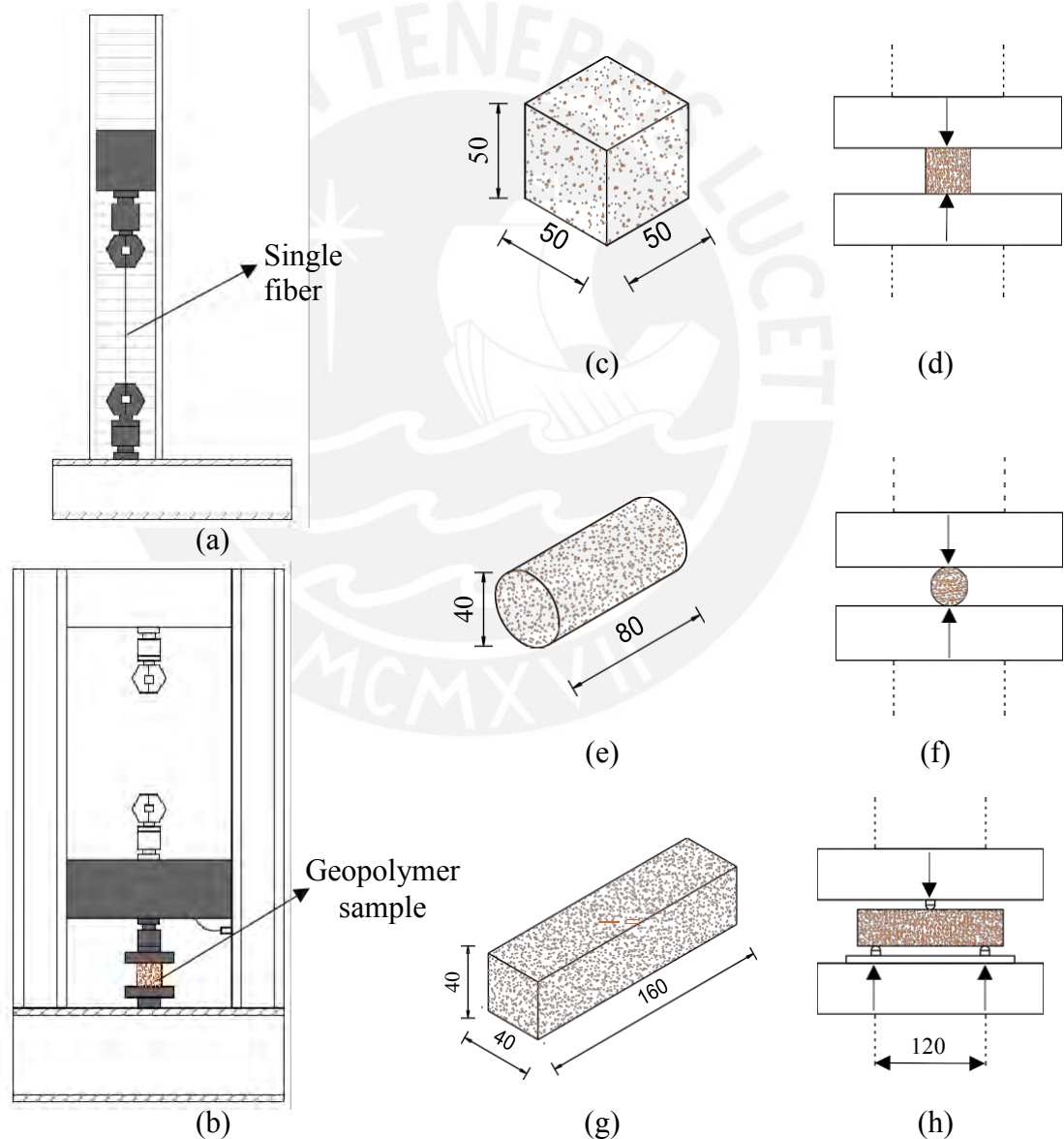


Figure 4.14. Mechanical characterization: (a) Tensile test of single fibers; (b) Universal testing machine used in mechanical characterization of geopolymer composites; (c) Geopolymer composite cubic sample; (d) Compression test; (e) Geopolymer composite cylindrical sample; (f) Splitting tensile test; (g) Geopolymer composite prismatic sample; (h) Three-point bending test. Units in mm.

4.2.3. Preparation of samples

Unreinforced geopolymer matrices (control matrices) and Fiber Reinforced Geopolymer Composites (FRGC) with jute and sisal fiber reinforcement were prepared to study their effect on the mechanical properties. Fired clay brick powder and the fibers were dry-mixed to ensure homogenous distribution. After that, the alkaline activating solution was gradually added and mixed until a homogenous paste was obtained with the aid of a mortar mixing machine type STJBJ-5. The alkaline activating solution had a $\text{SiO}_2/\text{Na}_2\text{O}$ molar ratio (M_s), Na_2O content and water/binder ratio of 0.60, 8% and 0.27, respectively (see details for activating solution optimization in ref. (G. Silva et al., 2019)). Figure 4.15 shows micrographs of the (a) control matrix, (b) jute-FRGC and (c) sisal-FRGC, immediately after mixing.

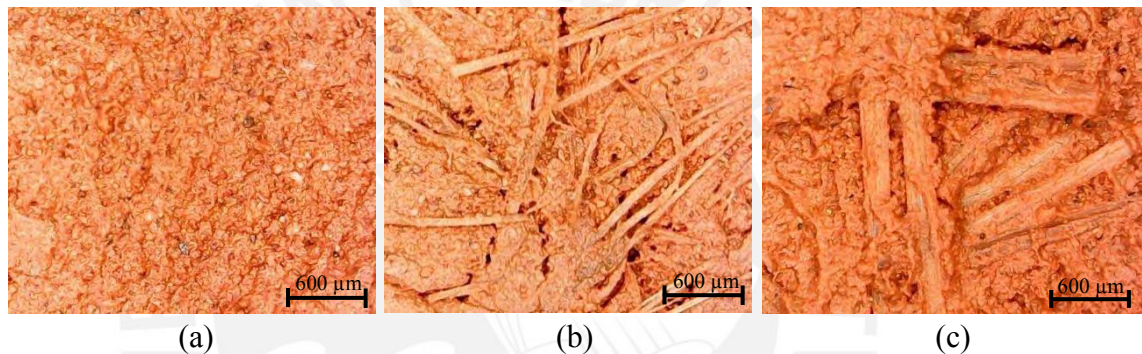


Figure 4.15. Micrographs of fresh geopolymer composites: (a) Control matrix; (b) Jute-FRGC; and (c) Sisal-FRGC.

Different contents of jute and sisal fibers in the reinforced composites were studied, these are expressed in terms of the weight ratio of each fiber to dry FCBP used in the mixture. Evaluated compositions varied from 0.5% to 2% in jute-FRGC and 0.5% to 3% in sisal-FRGC (a summary of the preparation conditions is presented in Table 3.12). The maximum quantities of the fibers were limited by the workability of the mixture. Addition of more water to counterbalance the loss of workability due to presence of the fibers was not considered in this study since reported data from other studies showed that addition of extra water decreased the mechanical properties of geopolymer matrices (Reig et al., 2013). For sample preparation, the geopolymer mixtures were hand-formed into the required shapes using cubic, cylindrical and prismatic silicon molds and were then subjected to vibration to remove trapped air bubbles. Specimens were cured in an oven at 65°C for 3 days (samples were de-molded after 24 hours, but kept in the oven) and then left at room temperature for four more days until mechanical tests were conducted. The oven curing time was limited to 3

days to avoid fiber degradation in FRGC. It is important to mention that specimens surfaces were painted white with black dots prior to mechanical testing.

Table 4.14. Summary of mixture proportions used for preparation of the control matrix and FRGCs.

Fiber type	Fiber addition (w/w, %)	Ms (mol/mol)	Na ₂ O (w/w, %)	Water/binder (w/w)	Oven temperature (°C)	Oven curing time (days)	Total curing time (days)
Control matrix	-	0.60	8	0.27	65	3	7
Jute	0.50	0.60	8	0.27	65	3	7
	1.00						
	1.50						
	2.00						
Sisal	0.50	0.60	8	0.27	65	3	7
	1.00						
	1.50						
	2.00						
	2.50						
	3.00						

4.3. Results and discussion

4.3.1. Tensile tests of fibers

Direct tensile tests were performed to determine the tensile strengths of single jute and sisal fibers. Tensile stresses were calculated as the ratio of the applied load and the transversal area of the fiber. The ratio between the crosshead displacements and the distance between grips were taken as the strain to develop the tensile stress vs strain curves. Six specimens of each type of fiber were tested under uniaxial tensile loads. Figure 4.16a shows the results of the tensile strength tests for both fibers. As can be seen, sisal fibers have more tensile strength than jute fibers, the tensile strength of sisal fibers was measured to be 508 MPa, while the strength of jute fibers was 276 MPa. The average tensile stress vs strain curves of both fibers are presented in Figure 4.16b. It can be observed that despite the difference in their tensile strengths, both fibers have similar modulus of elasticity (E-modulus). The value for the E-modulus for jute fibers was 27 GPa while sisal presented a slightly lower value of 25 GPa. However, sisal fibers presented 97% more elongation capacity than jute fibers as is shown in Figure 4.16b. The mechanical properties determined for both fibers were similar to the ones reported by Beukers & Van Hinte (2005).

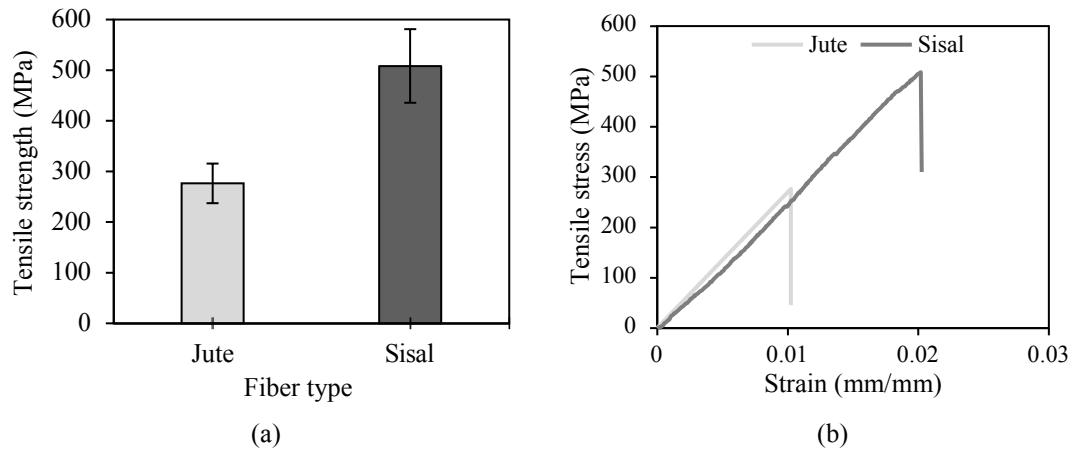


Figure 4.16. Tensile test of single jute and sisal fibers: (a) Tensile strengths; (b) Tensile stress vs strain curves.

4.3.2. Compression tests of geopolymer composites

Figure 4.17 shows the results of the uniaxial compression tests performed in the control samples and the FRGCs. Compression stresses were calculated as the ratio of the applied load and the transversal area of the 50 mm-cubic specimen. The ratio between the recorded displacements of the load cell and heights of the cubic specimen were considered as the strains to generate the compression stress-strain curves.

As shown in Figure 4.17a, the compressive strengths of both of the geopolymer composites exhibit an improved behavior when compared to the control sample. Moreover, the results indicate a trend, an increase in the strength with more fiber content, up to a limit where a decrease of the strength is observed. This maximum strength depends on the fiber type. In case of jute-FRGC, the 7th-day compressive strength presented a maximum of 20.6 MPa when the content of fibers was 1.5%, representing an increase of 64% with respect to the control. On the other hand, the sisal-FRGC samples with 2.5% fibers produced the highest increment (76%) on the 7th-day compressive strength with respect to the control matrix, reaching 22.1 MPa. It should be noted that higher fiber contents than the optimum proportion lead to a decrease in the compressive strength for both types of FRGC. Jute-FRGC with more fibers (2%) showed a lower compressive strength (19.0 MPa), while for sisal-FRGC, a 3% content of fibers decreased the compressive strength to 18.0 MPa. The average compression stress-strain curves for the control matrix, the optimum jute-FRGC (with a fiber content of 1.5%) and sisal-FRGC (2.5% fiber) are shown in Figure 4.17b. An increase of the E-modulus can be observed in both jute and sisal FRGCs with respect to

the control matrix, 103% for jute and 76% for sisal. The presence of both types of fibers changed significantly the way the samples broke apart during the compression tests. Figure 6c shows the brittle failure mode exhibited by the control matrix (no fiber-reinforcement), where small fragments are produced. On the other hand, the failure modes when jute and sisal fibers are present clearly show a more ductile behavior of the FRGCs (Figure 4.17d and 4.6e).

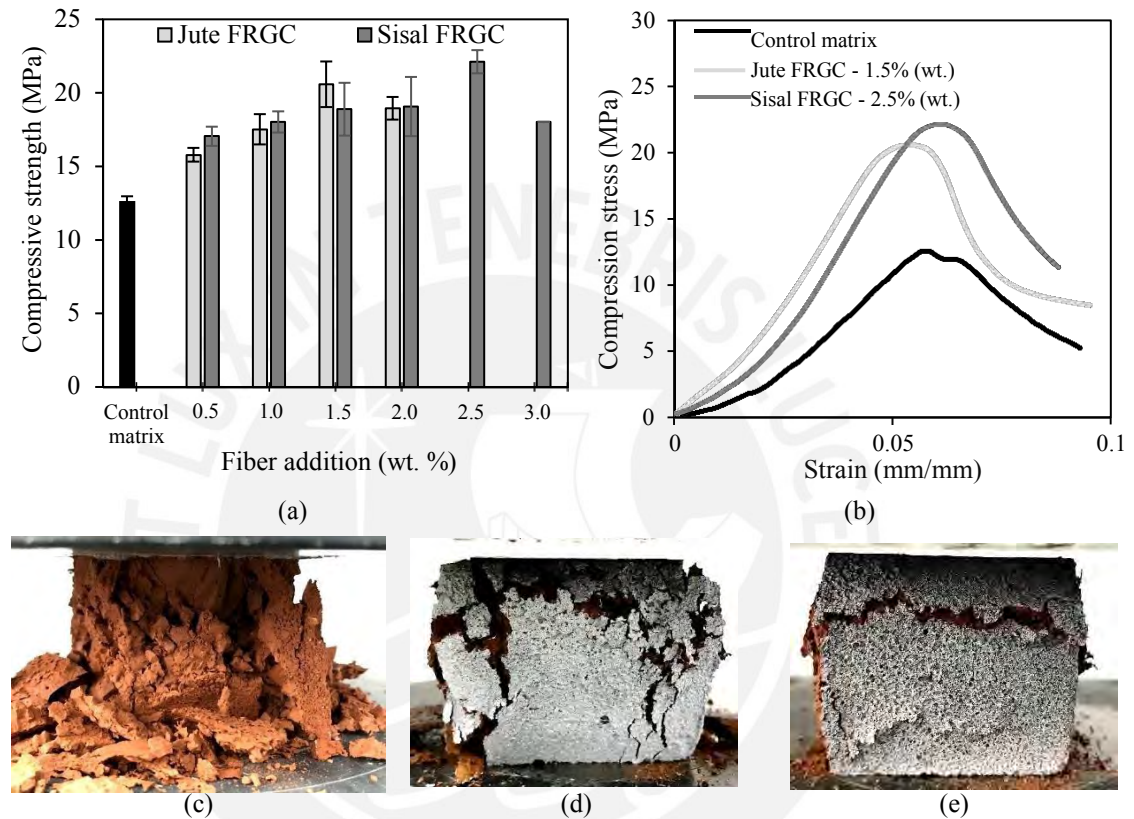


Figure 4.17. Compression test results for fiber-reinforced geopolymer composites: (a) 7th-day compressive strengths of specimens reinforced with jute and sisal fibers; (b) Compression vs. strain curves; (c) Failure mode of control matrix; (d) Failure mode of jute-FRGC (1.5% fiber content); and (e) Failure mode of sisal-FRGC (2.5% fiber content).

4.3.3. Splitting tests of geopolymer composites

Splitting tests were performed by applying a compression load along the longitudinal axis of the cylinder-shape samples. Tensile stresses were calculated using the following expression:

$$\sigma_s = \frac{2F}{\pi LD}$$

where F is the applied load while L and D denote length and diameter of the tested cylindrical sample.

The results of the splitting tests are shown in Figure 4.18. As can be seen, the addition of jute and sisal fibers improved the behavior of the tested matrices under tensile stresses. Similar to what was observed in the compression tests, both FRGCs showed an increase in the splitting tensile strength with more fiber content until reaching an optimum value. For jute-FRGCs, the highest splitting tensile strength (1.6 MPa) was obtained with addition of 1.5% fibers (the same optimum value obtained in the compression tests) surpassing in 45% the control matrix. In the case of sisal-FRGCs, with the addition of 2.5% fibers (also the same optimum value obtained in the compression tests) the tensile strength increased up to 2.3 MPa (112% higher than the control matrix). FRGCs with the optimum fiber content also exhibited a better tensile toughness in comparison to the control matrix (see Figure 4.18b). The tensile toughness was here defined as the area under the splitting tensile stress vs. displacement curve. 1.5% jute FRGC and 2.5% sisal FRGC presented an increment of 92% and 181% in the tensile toughness, respectively, with respect to the control matrix (1.4 kNm^{-1}). Finally, the splitting test of FRGCs also showed a more ductile failure mode in comparison to the control matrix (see Figure 4.18d and 4.7e). The behavior of FRGCs is characterized by multicracking due to the fact that the fibers allow the load transference from the cracked area to other uncracked parts of the sample. These results are in agreement with what was reported by other authors (Sun & Wu, 2008; Chen et al., 2014) regarding the transition from brittle to ductile behavior of fly ash based-geopolymer matrices by the addition of short fibers during splitting tests.

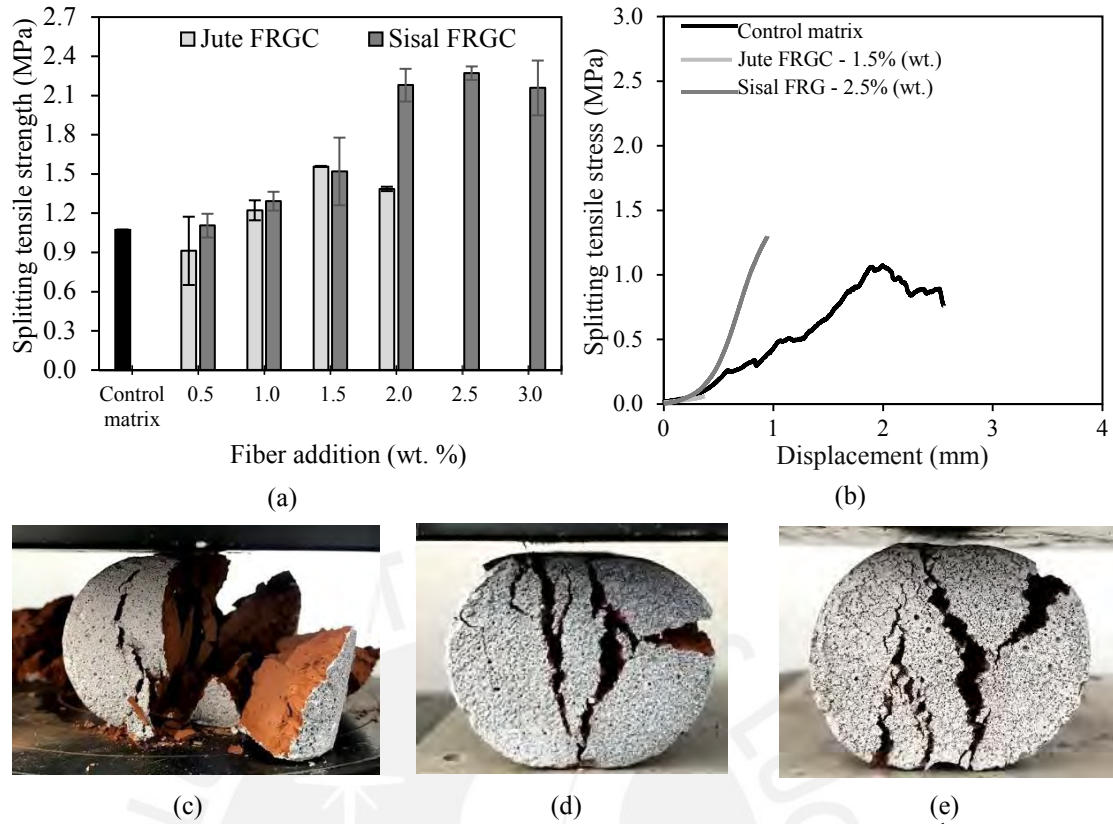


Figure 4.18. Splitting test results for fiber-reinforced geopolymer composites: (a) 7th-day splitting tensile strengths in specimens reinforced with jute and sisal fibers; (b) Tensile stress vs displacement curves; (c) Failure mode of control matrix; (d) Failure mode of jute-FRGC (1.5% fiber content); and (e) Failure mode of sisal-FRGC (2.5% fiber content).

4.3.4. Three-point bending tests of geopolymer composites

The control matrices and the jute and sisal FRGCs were subjected to three-point bending tests to evaluate their flexural strength and ultimate behavior. Flexural stress vs vertical displacement curves were plotted considering the applied force (F) and the mid-span vertical displacement of the load cell (which corresponds to the deflection measured at the mid-span of the specimen). Flexural stresses (σ_f) were calculated using the following equation:

$$\sigma_f = \frac{3FL}{2BH^2}$$

where F is the applied force, L denotes the free-span distance measured between the supporting points (120 mm for conducted tests), while H and B are the height and width of the prismatic specimens, respectively. On the other hand, the flexural modulus (E_f) was computed using the initial slope of the flexural stress vs. displacement curve ($\Delta F/\Delta X$), according to the following expression:

$$E_f = \frac{L^2}{6H} \left(\frac{\Delta \sigma_f}{\Delta X} \right)$$

The results of the three-point bending tests are presented in Figure 4.19. As shown, the influence of sisal and jute fiber reinforcement in the flexural response of the resulting geopolymer composites is evident. Unlike the results of compression and splitting tensile tests, a linear relationship between the flexural strength and the fiber content was observed for both types of FRGCs (Figure 4.19a). The flexural strengths of the samples with optimum fiber content for the previous compressive and tensile strengths were 1.6 MPa for jute-FRGC (1.5% fiber) and 2.2 MPa for sisal-FRGC (2% fiber), which correspond to an increase of 222% and 234%, respectively, in comparison to the flexural strength of the unreinforced FCBP-based geopolymer. However, these flexural strengths are not the highest for the studied FRGCs, for the three-point bending tests the maximum flexural strength is achieved with the highest fiber content. As mentioned before, the maximum amount of fiber in FRGCs was limited by the workability and homogeneity of the samples. For jute-FRGCs, the highest flexural strength, 3.3 MPa, was obtained with a fiber content of 2%, this represents an increase of 329% with respect to the control matrix. On the other hand, the addition of 3% of sisal fibers to the geopolymer matrix lead to an increase of the flexural strength of 360% with respect to the control matrix, reaching 3.5 MPa. It has been proposed that the improvement of the flexural strength observed in the FRGCs is because the fibers help to carry more tensile loads across cracks, as reported by Sun et al. (2008) and Chen et al. (2014). The effect of this can also be observed in Figure 4.19f, where fibers can be seen attached to both sides of the cracked sample. The failure modes of the control matrix, 2% jute-FRGC and 3% sisal-FRGC at the ultimate state are shown in Figure 4.19c, 4.8d and 4.8e, respectively. As it is apparent, the addition of both fibers causes a significant change in the failure behavior, going from an abrupt brittle crack to a controlled and more cohesive failure when the specimens are reinforced with fibers. Even though the response of the control matrix, 2% jute-FRGC and 3% sisal-FRGC under flexural loads in terms of the flexural strength and failure modes are very different, flexural stress vs. displacement curves (Figure 4.19b) showed that the flexural modulus of the control matrix and FRGCs are roughly similar (~ 90 MPa).

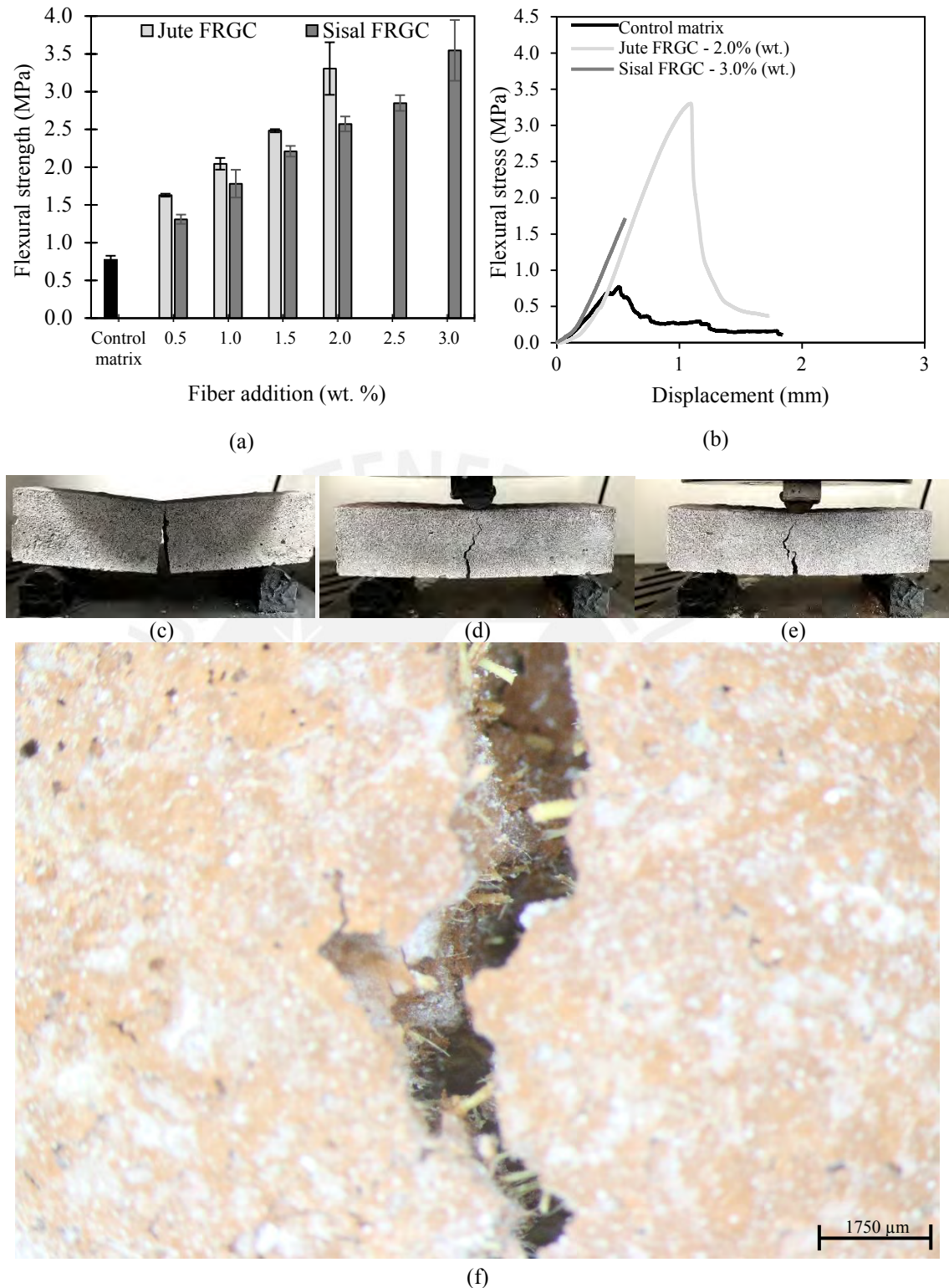
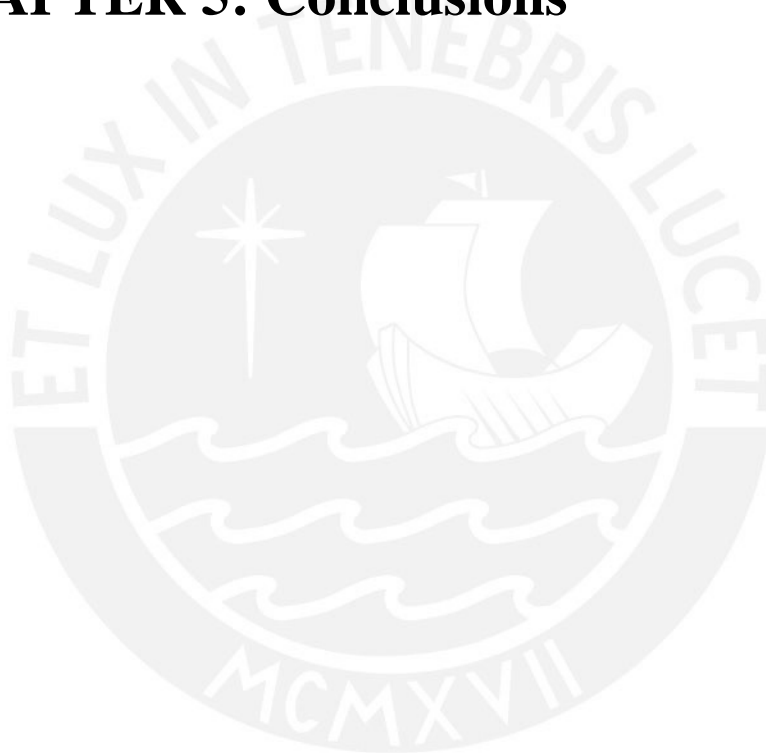


Figure 4.19. Three-point bending test results of fiber reinforced geopolymer composites: (a) 7th-day flexural strengths in specimens reinforced with jute and sisal fibers; (b) Flexural stress vs displacement curves; (c) Failure mode of control matrix; (d) Failure mode of jute-FRGC (2% fiber content); (e) Failure mode of sisal-FRGC (3% fiber content); and (f) Bridging of fibers across crack in sisal-FRGC (3% fiber content).

CHAPTER 5: Conclusions



5.1. Conclusions

The conclusions of the present work are addressed next with respect to different aspects, namely the review of the recent advances in natural fibers reinforced geopolymers, the optimization of the production conditions of FCBP-based geopolymers and the use of natural fibers as reinforcement of FCBP-based geopolymer composites.

Natural fibers reinforced geopolymers – A review of eco-friendly applications in the construction industry

This chapter has presented a review of a wide range of research studies that involve different geopolymer pastes and mortars, and also their reinforcement with fibers. All the materials that have been reported have the potential to be developed into eco-friendly construction materials since their silico-aluminate raw materials are industrial by-products or wastes, and the fibers for reinforcement are renewable and easily available since they are obtained mainly from plants. Studies involving geopolymer production from raw materials like fly ash, GGFBS, clay brick powder, concrete demolition waste, and mine tailings can show good mechanical properties that are comparable to OPC products. Furthermore, some studies have shown an improvement in the mechanical properties when combinations of silico-aluminate sources were used in the geopolymer synthesis. Morphology, size, and the molar ratio of $\text{SiO}_2/\text{Al}_2\text{O}_3$ in the raw material, together with the alkaline solution/solid ratio, NaOH concentration, $\text{SiO}_2/\text{M}_2\text{O}$ molar ratio in the total alkaline solution and the curing conditions have shown to be key parameters in the formulation of geopolymers in order to produce good mechanical properties. Available data show that these parameters need to be adapted to the raw material used. The review of the scientific literature shows that the fiber content and length in reinforcement affect the different mechanical strengths of the resulting reinforced geopolymer. Geopolymer matrices reinforced with natural fibers such as sweet sorghum, wool, cotton, sisal, and coir result in materials with increased compressive, flexural and tensile strengths and form a material with improved ductile behavior. Moreover, the reinforcement of geopolymer matrices can also be achieved with a layered approach by adding natural fiber bundles and fabrics to allow the development of a reinforced layered composite material with improved mechanical properties that depend mainly on the number of woven or non-woven

layers and the fabrication technique. In conclusion, the key parameters that need to be considered in the formulation of geopolymers were compiled and compared according to their composition, fabrication and resulting mechanical properties. Based on the reviewed information, it is evident that more research needs to be performed to help optimize formulations for the production of fiber-reinforced geopolymers with improved properties.

Analysis of the production conditions of geopolymer matrices from recycled construction and demolition wastes

The optimization of the production process of FCBP and NP-based geopolymers was carried out by analyzing the influence of five key parameters: Na₂O content, M_s, water/binder ratio, curing temperature and curing time. Based on the experimental results, the following conclusions can be drawn:

1. The Na₂O content and the M_s ratio affect the compressive strength of the resulting geopolymers. Variations in the Na₂O content significantly affect the 7th-day compressive strength as well as the setting time during mixing. An 8 % Na₂O content resulted in the highest compressive strength for both geopolymer matrices, lower and higher values of Na₂O content produce materials of lower compressive strengths. In addition, density values of FBCP-based geopolymers increase as the Na₂O content increases.
2. A decrease in the water/binder ratio from 0.29 to 0.27 led to a significant increase in the compressive strength of FCBP-based geopolymers. However, lower values of water/binder ratio resulted in lower compressive strengths which may be due to the presence of unreacted FCBP in the resulting product.
3. Oven curing time and temperature are the parameters that influenced the most the compressive strength of both geopolymers matrices. Unlike other silico-aluminate sources such as fly ash, it is apparent that both, FCBP needs more time to cure at high temperatures, this is, to polymerize and reach good mechanical properties. Experimental findings indicate that higher compressive strengths are achieved with moderate heating, at 65°C and 80°C, with longer curing times.
4. In this research, alternative and green cementitious materials with good mechanical properties and high potential for structural purposes have been developed using FCBP, a construction and demolition waste. A compressive strength of 36.6 ± 3.4

MPa was achieved after the optimization of the production conditions. The optimum alkaline solution for FCBP consisted of $M_s = 0.60$, Na_2O content of 8%, water/binder ratio = 0.27 with curing conditions between 65-80°C for 7 days.

Natural cellulose fibers to improve the mechanical behavior of fired clay brick-based geopolymer composites

Short natural jute and sisal fibers were able to reinforce fired clay brick powder-based geopolymers. The type and amount of fiber with respect to FCBP determines the properties of the resulting fiber reinforced geopolymer composites. Jute-FRGC with a 1.5% (by weight) fiber content showed the largest increase in compressive and tensile strengths, 64% and 45%, respectively, in comparison to the unreinforced FCBP-based geopolymer. For sisal-FRGCs, a content of 2.5% fibers showed the best performance increasing the compressive strength in 76% and the tensile strength in 112%, with respect to the unreinforced geopolymer. The addition of the fibers promoted a more ductile behavior and a less brittle rupture of the samples which were evident in all the stress-strain curves and the observation of the failure mode of the specimens. Three-point bending tests showed a linear relationship between the flexural strength of FRGCs and the natural fiber content. The flexural strength of jute-FRGC with 2% fiber content was 3.3 MPa, which corresponds to an increment of 329% in comparison to the unreinforced matrix. Similarly, sisal-FRGCs showed the best performance with a 3% fiber content showing a flexural strength of 3.5 MPa (a 360% improvement with respect to the unreinforced FCBP-based geopolymer).

References

- Abdullah, M., Faris, M., Tahir, M., Kadir, A., Sandu, A., Mat, N., & Corbu, O. (2017). Performance and Characterization of Geopolymer Concrete Reinforced with Short Steel Fiber. *IOP Conference Series: Materials Science and Engineering*, 209, 012038.
- Ahmari, S., Ren, X., Toufigh, V., & Zhang, L. (2012). Production of geopolymeric binder from blended waste concrete powder and fly ash. *Construction and Building Materials*, 35, 718–729.
- Ahmari, S., Zhang, L., & Zhang, J. (2012). Effects of activator type/concentration and curing temperature on alkali-activated binder based on copper mine tailings. *Journal of Materials Science*, 47(16), 5933–5945.
- Allahverdi, A., Mehrpour, K., & Kani, N. (2008). Taftan pozzolan-based geopolymer cement. *IUST International Journal of Engineering Science*, 19(3), 1–5.
- Allahverdi, A., Mehrpour, K., & Najafikani, E. (2008). Investigating the possibility of utilizing pumice-type natural pozzolan in production of geopolymer cement. *Ceramics - Silikaty*, 52(1), 16–23.
- Allahverdi, A., & Najafi, E. (2009). Construction Wastes as Raw Materials for Geopolymer Binders. *International Journal of Civil Engineering*, 7(3), 249–257.
- Alomayri, T., Shaikh, F., & Low, I. (2013a). Characterisation of cotton fibre-reinforced geopolymer composites. *Composites: Part B*, 50, 1–6.
- Alomayri, T., Shaikh, F., & Low, I. (2013b). Thermal and mechanical properties of cotton fabric-reinforced geopolymer composites. *Journal of Materials Science*, 48(19), 6746–6752.
- Alomayri, T., Shaikh, F., & Low, I. (2014a). Effect of fabric orientation on mechanical properties of cotton fabric reinforced geopolymer composites. *Materials and Design*, 57, 360–365.
- Alomayri, T., Shaikh, F., & Low, I. (2014b). Synthesis and mechanical properties of cotton fabric reinforced geopolymer composites. *Composites Part B: Engineering*, 60, 36–42.

- Alzeer, M., & Mackenzie, K. (2013). Synthesis and mechanical properties of novel composites of inorganic polymers (geopolymers) with unidirectional natural flax fibres (phormium tenax). *Applied Clay Science*, 75–76, 148–152.
- Alzeer, M., & MacKenzie, K. (2012). Synthesis and mechanical properties of new fibre-reinforced composites of inorganic polymers with natural wool fibres. *Journal of Materials Science*, 47(19), 6958–6965.
- American Coal Ash Association. (2015). *Coal Ash Production and Use Survey 2014*. Washington DC.
- ASTM International (2010). ASTM 618-17a, Standard Specification For Coal Fly Ash And Raw Or Calcined Natural Pozzolona For Use In Concrete. West Conshohocken, PA.
- Ardanuy, M., Claramunt, J., & Toledo, R. (2015). Cellulosic fiber reinforced cement-based composites: A review of recent research. *Construction and Building Materials*, 79, 115–128.
- Assaedi, H., Alomayri, T., Shaikh, F., & Low, I. (2015). Characterisation of mechanical and thermal properties in flax fabric reinforced geopolymer composites. *Journal of Advanced Ceramics*, 4(4), 272–281.
- ASTM International. (1998). ASTM C348, Standard Test Method for Flexural Strength of Hydraulic-Cement Mortars. *Annual Book of ASTM Standards*, 04, 2–7. West Conshohocken, PA.
- ASTM International. (2001). ASTM D3822-01, Standard Test Method for Tensile Properties of Single Textile Fibers. West Conshohocken, PA.
- ASTM International. (2016). ASTM C109/C109M – 16a, Standard Test Method for Compressive Strength of Hydraulic Cement Mortars (Using 2-in . or [50-mm] Cube Specimens). West Conshohocken, PA.
- ASTM International. (2017). ASTM C496 / C496M-17, Standard Test Method for Splitting Tensile Strength of Cylindrical Concrete Specimens,. West Conshohocken, PA.
- Atiş, C., Görür, E., Karahan, O., Bilim, C., Ilkentapar, S., & Luga, E. (2015). Very high strength (120 MPa) class F fly ash geopolymer mortar activated at different

- NaOH amount, heat curing temperature and heat curing duration. *Construction and Building Materials*, 96, 673–678.
- Ay, N., & Ünal, M. (2000). Use of waste ceramic tile in cement production. *Cement and Concrete Research*, 30(3), 497–499.
- B. Arisoy. (2002). *Development and fracture evaluation of high performance fiber reinforced lightweight concrete. PhD thesis. Wayne State University.*
- Barbosa, V. (1999). *Síntese e caracterização de polissialatos, Tese de doutorado. Instituto Militar de Engenharia, IME/RJ, Rio de Janeiro*
- Baronio, G., & Binda, L. (1997). Study of the pozzolanicity of some bricks and clays. *Construction and Building Materials*, 11(1), 41–46.
- Bentur, A., & Mindess, S. (2006). *Fiber reinforced cementitious composite* (2nd ed.). New York: CRC Press.
- Beukers, A., & Van Hinte, E. (2005). *Lightness: The inevitable renaissance of minimum energy structures*. Rotterdam: 010 publishers.
- Bing-hui, M., Zhu, H., Xue-min, C., Yan, H., & Si-yu, G. (2014). Applied Clay Science Effect of curing temperature on geopolymerization of metakaolin-based geopolymers. *Applied Clay Science*, 99, 144–148.
- Błaszczczyński, T., & Król, M. (2017). Alkaline Activator Impact on the Geopolymer Binders. *IOP Conference Series: Materials Science and Engineering*, 245(2).
- Böhmer, S., Neubauer, C., Schachermayer, E., Winter, B., & Walter, B. (2008). *Aggregates Case Study: Data gathering. Final Report referring to contract n° 150787-2007 FISC-AT*. Vienna.
- Brus, J., Abbrent, S., Kobera, L., Urbanova, M., & Cuba, P. (2016). Advances in ²⁷Al MAS NMR Studies of Geopolymers. In *Annual Reports on NMR Spectroscopy* (Vol. 88, pp. 79–147). Elsevier Ltd.
- Catauro, M., Papale, F., Lamanna, G., & Bollino, F. (2015). Geopolymer/PEG Hybrid Materials Synthesis and Investigation of the Polymer Influence on Microstructure and Mechanical Behavior. *Materials Research*, 18(4), 698–705.
- Chandramohan, D., & Marimuthu., K. (2011). A review on natural fibers.

- International Journal of Research and Reviews in Applied Sciences*, 8(2), 194–206.
- Chen, R., Ahmari, S., & Zhang, L. (2014). Utilization of sweet sorghum fiber to reinforce fly ash-based geopolymer. *Journal of Materials Science*, 49, 2548–2558.
- Cheng, T., & Chiu, J. (2003). Fire-resistant geopolymer produced by granulated blast furnace slag. *Minerals Engineering*, 16(3), 205–210.
- Chindaprasirt, P., & Chareerat, T. (2010). High-strength geopolymer using fine high-calcium fly ash. *Journal of Materials in Civil Engineering*, 23(3), 264–271.
- Chindaprasirt, P., Jaturapitakkul, C., Chalee, W., & Rattanasak, U. (2009). Comparative study on the characteristics of fly ash and bottom ash geopolymers. *Waste Management*, 29(2), 539–543.
- Correia, E., Torres, S., Alexandre, M., Gomes, K., Barbosa, N., & Barros, S. (2013). Mechanical Performance of Natural Fibers Reinforced Geopolymer Composites. *Materials Science Forum*, 758, 139–145.
- Das, S., Mohapatra, A., & Rath, A. (2014). Geo-polymer Concrete–Green Concrete for the Future—A Review. *International Journal of Civil Engineering Research*, 5(1), 2278–3652.
- Davidovits, J. (1979). Synthesis of new high-temperature geo-polymers for reinforced plastics/composites. In *Proc. SPE PACTEC'79 (Society of Plastic Engineers)* (pp. 151–154). Brookfield Center, USA.
- Davidovits, J. (1989). Geopolymers and geopolymeric materials. *Journal of Thermal Analysis*, 35(2), 429–441.
- Davidovits, J. (1991). Geopolymers: Inorganic Polymeric New Materials. *Journal of Thermal Analysis*, 37(8), 1633–1656.
- Davidovits, J. (1993). Carbon-Dioxide Greenhouse-Warming: What Future for Portland Cement. In *Proc. Emerging Technologies Symposium on Cement and Concretes in the Global Environment* (p. 21). Chicago, Illinois: Portland Cement Association.

- Davidovits, J. (1994). Properties of Geopolymer Cements. In *Proc. First International Conference on Alkaline Cements and Concretes* (pp. 131–149).
- Davidovits, J. (2005). The polysialate terminology: a very useful and simple model for the promotion and understanding of green-chemistry. In *Proc. Geopolymer, Green Chemistry and Sustainable Development Solutions* (pp. 9–12). Saint-Quentin: France.
- Dias, D., & Thaumaturgo, C. (2005). Fracture toughness of geopolymeric concretes reinforced with basalt fibers. *Cement and Concrete Composites*, 27(1), 49–54.
- Diaz, E., Allouche, E., & Eklund, S. (2010). Factors affecting the suitability of fly ash as source material for geopolymers. *Fuel*, 89(5), 992–996.
- Djobo, J. N. Y., Elimbi, A., Tchakouté, H. K., & Kumar, S. (2016). Reactivity of volcanic ash in alkaline medium, microstructural and strength characteristics of resulting geopolymers under different synthesis conditions. *Journal of Materials Science*, 51(22), 10301–10317.
- Duxson, P., & Provis, J. L. (2008). Designing precursors for geopolymer cements. *Journal of the American Ceramic Society*, 91(12), 3864–3869.
- European Committee for Standardization. (2008). Fly Ash For Concrete - Part 1: Definition, Specifications And Conformity Criteria. EN 450-1:2005+A1.
- Fernández-Jiménez, A., & Palomo, A. (2003). Characterisation of fly ashes. Potential reactivity as alkaline cements. *Fuel*, 82(18), 2259–2265.
- Food and Agriculture Organization of the United Nations (FAO). (2010). Future fibres.
- Gamarra, P., & Salhofer, S. (2007). A comparison of waste management in Peru and some Latin-American countries: an overview of major problems, characteristics and needs in the Region. In *“Management of Solid Wastes in Developing Countries.”* CISA Publisher.
- Gartner, E. (2004). Industrially interesting approaches to “low-CO₂” cements. *Cement and Concrete Research*, 34(9), 1489–1498.
- Ghosh, S., & Ghosh, S. (2015). Construction and Demolition Waste. In *Sustainable Solid Waste Management* (pp. 511–547).

- Gorkum, C. Van. (2010). *CO2 emissions and energy consumption during the construction of concrete structures*. Delft University of Technology, Delft.
- Guo, X., Shi, H., & Dick, W. (2010). Compressive strength and microstructural characteristics of class C fly ash geopolymer. *Cement and Concrete Composites*, 32(2), 142–147.
- He, J., Jie, Y., Zhang, J., Yu, Y., & Zhang, G. (2013). Synthesis and characterization of red mud and rice husk ash-based geopolymer composites. *Cement and Concrete Composites*, 37(1), 108–118.
- Hejazi, S., Sheikhzadeh, M., Abtahi, S., & Zadhoush, A. (2012). A simple review of soil reinforcement by using natural and synthetic fibers. *Construction and Building Materials*, 30, 100–116.
- Imbabi, M., Carrigan, C., & McKenna, S. (2012). Trends and developments in green cement and concrete technology. *International Journal of Sustainable Built Environment*, 1(2), 194–216.
- Islam, A., Alengaram, U., Jumaat, M., & Bashar, I. (2014). The development of compressive strength of ground granulated blast furnace slag-palm oil fuel ash-fly ash based geopolymer mortar. *Materials and Design*, 56, 833–841.
- Jawaid, M., & Abdul, H. (2011). Cellulosic/synthetic fibre reinforced polymer hybrid composites: A review. *Carbohydrate Polymers*, 86(1), 1–18.
- Jian-xiong, C., Han-bin, C., Pei, X., & Lan-fang, Z. (2004). A Study on Complex Alkali-Slag Environmental Concrete. In *International workshop on sustainable development and concrete technology* (pp. 299–307). Beijing.
- Khale, D., & Chaudhary, R. (2007). Mechanism of geopolymerization and factors influencing its development: A review. *Journal of Materials Science*, 42(3), 729–746.
- Komnitsas, K., Zaharaki, D., Vlachou, A., Bartzas, G., & Galetakis, M. (2015). Effect of synthesis parameters on the quality of construction and demolition wastes (CDW) geopolymers. *Advanced Powder Technology*, 26(2), 368–376.
- Kong, D., Sanjayan, J., & Sagoe-Crentsil, K. (2007). Comparative performance of geopolymers made with metakaolin and fly ash after exposure to elevated

- temperatures. *Cement and Concrete Research*, 37(12), 1583–1589.
- Korniejenko, K., Fraczek, E., Pytlak, E., & Adamski, M. (2016). Mechanical properties of geopolymer composites reinforced with natural fibers. *Procedia Engineering*, 151, 388–393.
- Korniejenko, K., Mikuła, J., & Łach, M. (2015). Fly Ash Based Fiber-Reinforced Geopolymer Composites as the Environmental Friendly Alternative to Cementitious Materials. In *Proc. 2015 International Conference on Bio-Medical Engineering and Environmental Technology* (pp. 164–171).
- Krishnan, L., Karthikeyan, S., Nathiya, S., & Suganya, K. (2014). Geopolymer Concrete an Eco-Friendly Construction Material. *International Journal of Research in Engineering and Technology*, 3(11), 164–167.
- Kriven, W., Bell, J., & Gordon, M. (2003). Geopolymer Refractories for the Glass Manufacturing Industry. In *Proc. 64th Conference on Glass Problems* (pp. 57–79).
- Kriven, W., Keane, P., & Musil, S. (2013). Green composite: Sodium-based geopolymer reinforced with chemically extracted corn husk fibers. *Developments in Strategic Materials and Computational Design IV*, 123–133.
- Lampris, C., Lupo, R., & Cheeseman, C. (2009). Geopolymerisation of silt generated from construction and demolition waste washing plants. *Waste Management*, 29(1), 368–373.
- Lau, A., & Hung, A. (2017). *Natural Fiber-Reinforced Biodegradable and Bioresorbable Polymer Composites*. (A. Lau & A. Hung, Eds.). Duxford: Woodhead Publishing.
- Lee, W. K. W., & Van Deventer, J. S. J. (2003). Use of Infrared Spectroscopy to Study Geopolymerization of Heterogeneous Amorphous Aluminosilicates. *Langmuir*, 19(21), 8726–8734.
- Li, W., & Xu, J. (2009). Impact characterization of basalt fiber reinforced geopolymeric concrete using a 100-mm-diameter split Hopkinson pressure bar. *Materials Science and Engineering A*, 513–514(C), 145–153.
- Li, Y., Mai, Y., & Ye, L. (2006). Sisal fibre and its composites: a review of recent

- developments. *Composites Science and Technology*, 60(2000), 2037–2055.
- Lin, T., Jia, D., He, P., Wang, M., & Liang, D. (2008). Effects of fiber length on mechanical properties and fracture behavior of short carbon fiber reinforced geopolymer matrix composites. *Materials Science and Engineering A*, 497, 181–185.
- Marzouk, M., & Azab, S. (2014). Environmental and economic impact assessment of construction and demolition waste disposal using system dynamics. *Resources, Conservation and Recycling*, 82, 41–49.
- Matheu, P., Ellis, K., & Varela, B. (2015). Comparing the environmental impacts of alkali activated mortar and traditional portland cement mortar using life cycle assessment. *IOP Conference Series: Materials Science and Engineering*, 96(1), 4–11.
- Ministerio de Fomento de España. (2010). *Actualización del catálogo de residuos utilizables en construcción*.
- Mohanty, A., Misra, M., & Drzal, L. (2005). *Natural Fibers, Biopolymers, and Biocomposites*. Boca Raton: Taylor & Francis Group.
- Monier, V., Hestin, M., Trarieux, M., Mimid, S., Domrose, L., Van Acoleyen, M., ... Mudgal, S. (2011). *Study on the Management of Construction and Demolition Waste in the EU. Contract 07.0307/2009/540863/SER/G2, Final report for the European Commission (DG Environment)*.
- Natali, A., Manzi, S., & Bignozzi, M. (2011). Novel fiber-reinforced composite materials based on sustainable geopolymer matrix. *Procedia Engineering*, 21, 1124–1131.
- Natural Resources Canada. (2013). *Tailings Management at NRCan*. Ottawa.
- Nehdi, M., & Khan, A. (2004). Protective System for Buried Infrastructure Using Recycled Tire Rubber-Filled Cement Mortars. *Special Publication*, 219, 99–114.
- NPCS Board of Consultants & Engineers. (2008). *The Complete Technology Book on Minerals & Mineral Processing*. Delhi: Asia Pacific Business Press Inc.
- Oh, J., Monteiro, P., Jun, S., Choi, S., & Clark, S. (2010). The evolution of strength

- and crystalline phases for alkali-activated ground blast furnace slag and fly ash-based geopolymers. *Cement and Concrete Research*, 40(2), 189–196.
- Omer, S., Demirboga, R., & Khushefati, W. (2015). Relationship between compressive strength and UPV of GGBFS based geopolymer mortars exposed to elevated temperatures. *Construction and Building Materials*, 94, 189–195.
- Pacheco-Torgal, F., Castro-Gomes, J., & Jalali, S. (2009). Tungsten mine waste geopolymeric binder: Preliminary hydration products investigations. *Construction and Building Materials*, 23(1), 200–209.
- Pacheco-torgal, F., & Jalali, S. (2011). Cementitious building materials reinforced with vegetable fibres: A review. *Construction and Building Materials*, 25(2), 575–581.
- Pacheco-Torgal, F., & Jalali, S. (2010a). Influence of sodium carbonate addition on the thermal reactivity of tungsten mine waste mud based binders. *Construction and Building Materials*, 24(1), 56–60.
- Pacheco-Torgal, F., & Jalali, S. (2010b). Reusing ceramic wastes in concrete. *Construction and Building Materials*, 24(5), 832–838.
- Pacheco-Torgal, F., & Jalali, S. (2012). Earth construction: Lessons from the past for future eco-efficient construction. *Construction and Building Materials*, 29, 512–519.
- Palomo, A., Grutzeck, M., & Blanco, M. (1999). Alkali-activated fly ashes: A cement for the future. *Cement and Concrete Research*, 29(8), 1323–1329.
- Pan, N. C., Day, A., & Mahalanabis, K. K. (1999). Chemical composition of jute and its estimation. *Man-Made Textiles in India*, 42, 467–473.
- Panagiotopoulou, C., Tsivilis, S., & Kakali, G. (2015). Application of the Taguchi approach for the composition optimization of alkali activated fly ash binders. *Construction and Building Materials*, 91, 17–22.
- Pathak, A., Kumar, S., & Jha, V. (2014). Development of Building Material from Geopolymerization of Construction and Demolition Waste (CDW). *Transactions of the Indian Ceramic Society*, 73(2), 133–137.

- Pernica, D., Reis, P., Ferreira, J., & Louda, P. (2010). Effect of test conditions on the bending strength of a geopolymer-reinforced composite. *Journal of Materials Science*, 45(3), 744–749.
- Pickering, K., Efendy, M., & Le, T. (2016). A review of recent developments in natural fibre composites and their mechanical performance. *Composites Part A: Applied Science and Manufacturing*, 83, 98–112.
- Pradeep, K., & Rakesh, K. (2012). Studies on Water Absorption of Bamboo-Epoxy Composites: Effect of Silane Treatment of Mercerized Bamboo. *Journal of Composite Materials*, 21(7), 449–456.
- Provis, J. L., Harrex, R. M., Bernal, S. A., Duxson, P., & Van Deventer, J. S. J. (2012). Dilatometry of geopolymers as a means of selecting desirable fly ash sources. *Journal of Non-Crystalline Solids*, 358(16), 1930–1937.
- Provis, J., Yong, C., Duxson, P., & Van Deventer, J. (2009). Correlating mechanical and thermal properties of sodium silicate-fly ash geopolymers. *Colloids and Surfaces A: Physicochemical and Engineering Aspects*, 336(1–3), 57–63.
- Puertas, F., Amat, T., Fernández-Jiménez, A., & Vázquez, T. (2003). Mechanical and durable behaviour of alkaline cement mortars reinforced with polypropylene fibres. *Cement and Concrete Research*, 33(12), 2031–2036.
- Puertas, F., García-Díaz, I., Palacios, M., Gazulla, M., Gómez, M., & Orduña, M. (2010). Clinkers and cements obtained from raw mix containing ceramic waste as a raw material. Characterization, hydration and leaching studies. *Cement and Concrete Composites*, 32(3), 175–186.
- Querol, X., Moreno, N., Umaa, J., Alastuey, A., Hernández, E., López-Soler, A., & Plana, F. (2002). Synthesis of zeolites from coal fly ash: an overview. *International Journal of Coal Geology*, 50(1–4), 413–423.
- Rakhimova, N., & Rakhimov, R. (2015). Alkali-activated cements and mortars based on blast furnace slag and red clay brick waste. *Materials and Design*, 85, 324–331.
- Rattanasak, U., & Chindaprasirt, P. (2009). Influence of NaOH solution on the synthesis of fly ash geopolymer. *Minerals Engineering*, 22(12), 1073–1078.

- Rees, C. A., Provis, J. L., Lukey, G. C., & Van Deventer, J. S. J. (2007). Attenuated total reflectance fourier transform infrared analysis of fly ash geopolymer gel aging. *Langmuir*, 23(15), 8170–8179.
- Reig, L., Soriano, L., Borrachero, M., Monzó, J., & Payá, J. (2016). Influence of calcium aluminate cement (CAC) on alkaline activation of red clay brick waste (RCBW). *Cement and Concrete Composites*, 65, 177–185.
- Reig, L., Tashima, M., Borrachero, M., Monzó, J., Cheeseman, C., & Payá, J. (2013a). Properties and microstructure of alkali-activated red clay brick waste. *Construction and Building Materials*, 43, 98–106.
- Reig, L., Tashima, M., Soriano, L., Borrachero, M., Monzó, J., & Payá, J. (2013). Alkaline activation of ceramic waste materials. *Waste and Biomass Valorization*, 4(4), 729–736.
- Sá, R., Sá, M., Sankar, K., & Kriven, W. (2016). Geopolymer-bamboo composite – A novel sustainable construction material. *Construction and Building Materials*, 123, 501–507.
- Sakulich, A. (2011). Reinforced geopolymer composites for enhanced material greenness and durability. *Sustainable Cities and Society*, 1(4), 195–210.
- Salih, M., Abang, A., & Farzadnia, N. (2014). Characterization of mechanical and microstructural properties of palm oil fuel ash geopolymer cement paste. *Construction and Building Materials*, 65, 592–603.
- Salomons, W. (1995). Environmental impact of metals derived from mining activities: Processes, predictions, prevention. *Journal of Geochemical Exploration*, 52(1–2), 5–23.
- Schilling, P., Roy, A., Eaton, H., Malone, P., & Brabston, N. (2011). Microstructure, strength, and reaction products of ground granulated blast • furnace slag activated by highly concentrated NaOH solution. *Journal of Materials Research*, 9(1), 188–197.
- Shaikh, F. (2013). Review of mechanical properties of short fibre reinforced geopolymer composites. *Construction and Building Materials*, 43, 37–49.
- Silva, P. De, Sagoe-Crenstil, K., & Sirivivatnanon, V. (2007). Kinetics of

- geopolymerization: Role of Al₂O₃ and SiO₂. *Cement and Concrete Research*, 37(4), 512–518.
- Silva, F., Dias, R., de Almeida, J., & de Moraes, E. (2010). Physical and mechanical properties of durable sisal fiber-cement composites. *Construction and Building Materials*, 24(5), 777–785.
- Silva, G., Castañeda, D., Kim, S., Castañeda, A., Bertolotti, B., Ortega-San-Martin, L., Aguilar, R. (2019). Analysis of the production conditions of geopolymer matrices from natural pozzolan and recycled construction and demolition wastes, submitted to *Construction and Building Materials*.
- Silva, I., Castro-Gomes, J., & Albuquerque, A. (2012). Effect of immersion in water partially alkali-activated materials obtained of tungsten mine waste mud. *Construction and Building Materials*, 35, 117–124.
- Singh, B., Ishwarya, G., Gupta, M., & Bhattacharyya, S. (2015). Geopolymer concrete: A review of some recent developments. *Construction and Building Materials*, 85, 78–90.
- Somna, K., Jaturapitakkul, C., Kajitvichyanukul, P., & Chindaprasirt, P. (2011). NaOH-activated ground fly ash geopolymer cured at ambient temperature. *Fuel*, 90(6), 2118–2124.
- Sun, P., & Wu, H. (2008). Transition from brittle to ductile behavior of fly ash using PVA fibers. *Cement and Concrete Composites*, 30(1), 29–36.
- Temuujin, J., Williams, R., & Van Riessen, A. (2009). Effect of mechanical activation of fly ash on the properties of geopolymer cured at ambient temperature. *Journal of Materials Processing Technology*, 209(12–13), 5276–5280.
- Thomas, M. (2011). *Supplementary Cementing Materials in Concrete* (1st ed.). Boca Raton: CRC Press.
- U.S. Environmental Protection Agency (EPA). (2016). *Advancing sustainable materials management: 2014 fact sheet*. United States Environmental Protection Agency, Office of Land and Emergency Management, Washington, DC 20460. Washington DC.
- U.S. Geological Survey. (2017). *Mineral Commodity Summaries 2017: U.S.*

- Geological Survey*. Virginia: Interior Dept. Geological Survey.
- Vafaei, M., & Allahverdi, A. (2016). Influence of calcium aluminate cement on geopolymerization of natural pozzolan. *Construction and Building Materials*, *114*, 290–296.
- Van Oss, H. (2002). Slag - Iron and Steel. In *U.S. Geological Survey Minerals Yearbook—2002* (pp. 1–6).
- Vásquez, A., Cárdenas, V., Robayo, R., & de Gutiérrez, R. (2016). Geopolymer based on concrete demolition waste. *Advanced Powder Technology*, *27*(4), 1173–1179.
- Villa, C., Pecina, E., Torres, R., & Gómez, L. (2010). Geopolymer synthesis using alkaline activation of natural zeolite. *Construction and Building Materials*, *24*(11), 2084–2090.
- Wilson, D., Velis, C., & Cheeseman, C. (2006). Role of informal sector recycling in waste management in developing countries. *Habitat International*, *30*(4), 797–808.
- Xie, Y., Hill, C., Xiao, Z., Militz, H., & Mai, C. (2010). Silane coupling agents used for natural fiber/polymer composites: A review. *Composites Part A: Applied Science and Manufacturing*, *41*(7), 806–819.
- Yadollahi, M., Benli, A., & Demirboğa, R. (2015). The effects of silica modulus and aging on compressive strength of pumice-based geopolymer composites. *Construction and Building Materials*, *94*, 767–774.
- Yahya, Z., Abdullah, M., Hussin, K., Ismail, K., Razak, R., & Sandu, A. (2015). Effect of Solids-To-Liquids, Na₂SiO₃-To-NaOH and Curing Temperature on the Palm Oil Boiler Ash (Si + Ca) Geopolymerisation System. *Materials*, *8*(5), 2227–2242.
- Yan, L. (2012). Effect of alkali treatment on vibration characteristics and mechanical properties of natural fabric reinforced composites. *Journal of Reinforced Plastics and Composites*, *31*(13), 887–896.
- Yan, L., & Chouw, N. (2013). Behavior and analytical modeling of natural flax fibre-reinforced polymer tube confined plain concrete and coir fibre-reinforced concrete. *Journal of Composite Materials*, *47*(17), 2133–2148.

- Yan, L., Chouw, N., & Jayaraman, K. (2014). Lateral crushing of empty and polyurethane-foam filled natural flax fabric reinforced epoxy composite tubes. *Composites Part B: Engineering*, 63, 15–26.
- Yan, L., Kasal, B., & Huang, L. (2016). A review of recent research on the use of cellulosic fibres, their fibre fabric reinforced cementitious, geo-polymer and polymer composites in civil engineering. *Composites Part B: Engineering*, 92, 94–132.
- Yunsheng, Z., Wei, S., Zongjin, L., Xiangming, Z., Eddie, & Chungkong, C. (2008). Impact properties of geopolymer based extrudates incorporated with fly ash and PVA short fiber. *Construction and Building Materials*, 22(3), 370–383.
- Zawrah, M., Gado, R., Feltin, N., Ducourtieux, S., & Devoille, L. (2016). Recycling and utilization assessment of waste fired clay bricks (Grog) with granulated blast-furnace slag for geopolymer production. *Process Safety and Environmental Protection*, 103, 237–251.
- Zhang, L., Ahmari, S., & Zhang, J. (2011). Synthesis and characterization of fly ash modified mine tailings-based geopolymers. *Construction and Building Materials*, 25(9), 3773–3781.
- Zhang, Y., Sun, W., & Li, Z. (2008). Infrared spectroscopy study of structural nature of geopolymeric products. *Journal Wuhan University of Technology, Materials Science Edition*, 23(4), 522–527.
- Zhang, Z., Provis, J., Reid, A., & Wang, H. (2014). Geopolymer foam concrete: An emerging material for sustainable construction. *Construction and Building Materials*, 56, 113–127.
- Zhao, Q., Nair, B., Rahimian, T., & Balaguru, P. (2007). Novel geopolymer based composites with enhanced ductility. *Journal of Materials Science*, 42(9), 3131–3137.